# Mucin-degrading gut bacteria promote anti-parasitic immunity

**Short title:** *Nematodes and gut microbial mucin foraging*

Mathis Wolter[a,b], Marie Boudaud[a#], Erica T. Grant[a,b], Amy Parrish[a,b], Alessandro De Sciscio[a], Seona Thompson[c,d], Jean-Jacques Gerardy[e,f], Michel Mittelbronn[e,f,g,h,i,j], David J. Thornton[c,d], Andrew J. Macpherson[k,l,m], Richard K. Grencis[c,d] and Mahesh S. Desai[a,n,*]

[a]*Department of Infection and Immunity, Luxembourg Institute of Health, Esch-sur-Alzette, Luxembourg*

[b]*Faculty of Science, Technology and Medicine, University of Luxembourg, Esch-sur-Alzette, Luxembourg*

[c]*Lydia Becker Institute for Immunology and Inflammation. Faculty of Biology, Medicine and Health, University of Manchester, Manchester, United Kingdom*

[d]*Wellcome Centre for Cell Matrix Research, Faculty of Biology, Medicine and Health, University of Manchester, Manchester, United Kingdom*

[e]*National Center of Pathology, Laboratoire National de Santé, Dudelange, Luxembourg*

[f]*Luxembourg Center of Neuropathology, Dudelange, Luxembourg*

[g]*Luxembourg Centre for Systems Biomedicine, University of Luxembourg, Esch-sur-Alzette, Luxembourg*

[h]*Department of Cancer Research, Luxembourg Institute of Health, Luxembourg, Luxembourg*

[i]*Faculty of Science, Technology and Medicine, University of Luxembourg, Esch-sur-Alzette*

[j]*Department of Life Science and Medicine, University of Luxembourg, Esch-sur-Alzette, Luxembourg*

[k]*Department of Visceral Surgery and Medicine, Bern University Hospital, University of Bern, Bern, Switzerland*

[l]*Maurice Müller Laboratories, Department for Biomedical Research, University of Bern, Bern, Switzerland*

[m]*CMPG, Institute of Ecology and Evolution, University of Bern, Bern, Switzerland*

[n]*Odense Research Center for Anaphylaxis, Department of Dermatology and Allergy Center, Odense University Hospital, University of Southern Denmark, Odense, Denmark*

[#]These authors contributed equally

[*]Corresponding author: Mahesh S. Desai, mahesh.desai@lih.lu

**Grant support**

This work was supported by the following grants in the laboratory of M.S.D.: Luxembourg National Research Fund (FNR) CORE grants (C15/BM/10318186 and C18/BM/12585940) and BRIDGES grant (22/17426243) to M.S.D.; FNR PRIDE (17/11823097) and the Fondation du Pélican de Mie et Pierre Hippert- Faber, under the aegis of the Fondation de Luxembourg grants to E.T.G.; FNR AFR individual PhD fellowship to A.P. (11602973); and European Commission Horizon 2020 Marie Skłodowska-Curie Actions individual fellowship to M.B. (897408). MM thanks the Luxembourg National Research Fond (FNR) for the support (FNR PEARL P16/BM/11192868 grant). The Wellcome Trust supports work of R.K.G and S.T. (Z10661/Z/18/Z; 203128A/Z/16/Z) and D.J.T (203128A/Z/16/Z).

**Correspondence**

Mahesh S. Desai, PhD
Luxembourg Institute of Health
Department of Infection and Immunity
29, rue Henri Koch, L-4354 Esch-sur-Alzette
Luxembourg
Tel: +352 26970-389
Fax: +352 26970-390
Email: mahesh.desai@lih.lu

**Disclosures**

M.S.D. works as a consultant and an advisory board member at Theralution GmbH, Germany.

**Author Contributions**

M.S.D. supervised the study and obtained research funding; M.W., M. B., D.J.T., R.K.G. and M.S.D. conceived and designed the study; M.W., M. B., E.T.G., A.P., A.D.S., and S.T. performed the experiments; M.W., E.T.G., R.K.G., A.P. and M.B. analyzed the data; J.-J. G. and M.M. prepared slides for histology; A.J.M. supplied germ-free mice; M.W., M. B., and M.S.D. primarily wrote the manuscript. All authors reviewed and approved the manuscript.

**Data Transparency Statement**

All data, study materials and analytical methods will be made available to other researchers upon request.

## Abstract

**BACKGROUND & AIMS**

Host-secreted gastrointestinal mucus plays a key role in the expulsion of intestinal nematode parasites. A balance between mucin secretion by the host and the gut microbial mucin foraging is essential to maintain the intestinal homeostasis, yet little is known about how changes in the mucin–microbiome interactions affect worm infections. Here, we aimed to examine how mucin foraging activity by the microbiome changes the course of parasitic worm infections by modulating the host immune responses.

**METHODS**

We utilized a gnotobiotic mouse model containing a synthetic human gut microbiota that allows for: 1) a complete removal of the mucin-degrading bacteria from the community; and 2) diet-driven manipulation of the microbiota toward mucin foraging. We infected mice with a murine nematode, *Trichuris muris*, which resembles human infection with *Trichuris trichiura*. We examined the temporal dynamics of worm infection including worm burden and the host immune responses, and coupled these readouts to the microbial changes and mucin foraging activity.

**RESULTS**

The absence of mucin-degrading bacteria in the microbiota enhances susceptibility to parasitic infection—evidenced by higher worm number—by promoting stronger Th1 immune responses. Dietary fiber deprivation increases the microbial mucin-foraging activity, which coincides with a shift in host immune responses from susceptible (chronic, Th1 type) to resistant (acute, Th2 type), thereby promoting worm clearance.

**CONCLUSIONS**

Our results provide mechanistic insights into how the colonic mucin-degrading bacteria promote anti-parasitic immunity through modulation of the host immune responses. Our study documents a clinically-relevant, novel link in the microbiome–parasite–host immune axis that is useful prerequisite knowledge in managing parasitic infections.

**Keywords**

Mucin; gut microbiome; anti-parasitic immunity; nematode; *Trichuris muris*

## Introduction

Intestinal parasitic worms (helminths) make an invaluable model to study the host immunomodulatory mechanisms due to their ability to subvert the host immune responses[1]. In this context, the murine parasite *Trichuris muris*—a relevant biological model for the closely related human parasite *Trichuris trichiura*—has been extensively investigated[2]. *T. muris* is an especially attractive experimental model as either a susceptible or resistant immune response can be investigated[2,3]. Susceptibility in mice, which is more reflective of the naturally-occurring chronic infections[4], is generally characterized by a Th1 response resulting in long-term worm infections and chronic colitis. On the other hand, resistance is characterized by an acute Th2 response leading to worm clearance and tissue repair[2].

Since they occupy the same host environment, it is no surprise that enteric parasites such as helminths strongly interact with the gut microbiome[5,6]. Although these interactions may lead to the suppression of either the gut microbiome or the helminth[5–7], in case of *T. muris*, bacterial–helminth crosstalk is essential for worm hatching, as the parasite eggs fail to hatch and establish in germ-free environments[8–10]. Once the worm has settled in the intestinal epithelium, the bacterial–helminth dynamics appear mainly unidirectional, with helminths altering the microbiome composition through various mechanisms, including through helminth excretory-secretory products or host anti-microbial peptides, released in response to the parasite[11–15]. Furthermore, the helminths alter the nutrients available to the microbiome, indirectly influencing bacteria selection[16]. The effect of the infection on host immunology has an additional impact on the microbiome, as the worms or their metabolic byproducts can alter toll-like receptor (TLR) expression profiles[17,18] or responsiveness of host immune cells to TLR ligands[19] and interfere with local IgA-production[17]. While the gastrointestinal (GI) mucins are essential for worm clearance[20–22] and the impacts of the helminth infection on the microbiome during worm clearance are documented at the broader level of microbial phylogeny[23–28], questions remain regarding how the mucus–microbiome interactions are affected by and affect worm infection and the underlying host immune responses.

Worm expulsion during an acute response is largely driven by goblet-cell secreted gastrointestinal mucin that is tightly linked to the Th2-type immune response[22]. Along these lines, mice lacking the *Muc2* gene, which encodes the major glycoprotein of the GI mucus,

show a delayed clearance of *T. muris*[29] and *Muc5ac* deficient mice completely fail to clear the helminth[22].

We have previously shown that a fiber-deprived microbiota leads to a disrupted balance towards excessive gut microbial mucin foraging activity[30–32]. As the balance between mucin secretion and its consumption by the gut microbes is critical for intestinal homeostasis[33,34], here, we hypothesized that excessive mucin foraging by the microbiota alters the course of the parasite infection by modulating the immune response. To test this hypothesis, we employed a tractable 14-member synthetic human microbiota (14SM) characterized for the capability of individual members to degrade various glycans including mucin oligosaccharides[31,35]. In a longitudinal experimental setup, using ex-germ-free mice with a mucin-foraging or a non-mucin-foraging synthetic microbiota, we studied how mucin–gut microbiome interactions shape anti-parasitic immunity. Our findings suggest a mechanism of how mucin-degrading bacteria promote anti-parasitic immunity, which sheds a new light on the microbiome–parasite–host immune interactions.

## Methods

### *Ethical statement*

All animal experiments were performed according to the "Règlement Grand-Ducal du 11 janvier 2013 relatif à la protection des animaux utilisés à des fins scientifiques" based on Directive 2010/63/EU on the protection of animals used for scientific purposes, and approved by the Animal Experimentation Ethics Committee of the University of Luxembourg and by the Luxembourgish Ministry of Agriculture, Viticulture, and Rural Development (national authorization no. LUPA2020/02). The mice were housed in accordance with the recommendations stated by the Federation of European Laboratory Animal Science Associations (FELASA).

### *Experimental design and dietary treatment*

8–23 weeks old C57BL/6 mice were housed in ISOcages with up to five animals per cage. Sterile food and water were provided *ad libitum* and light cycles consisted of 12 hours. Before the administration of 14SM, the germ-free status of the mice was confirmed using aerobic and anaerobic culturing of stools samples. Mice were intragastrically gavaged with 0.2 ml of the 14SM or 10SM gavage mix as described previously[35]. Before and for 6–9 days following the

167 gavage, mice were maintained on a standard mouse chow, which we refer to as Fiber-rich (FR)
168 diet. Afterwards, half of the mice were assigned to a Fiber-free (FF) diet and the rest remained
169 on the FR diet. Twenty days after the diet switch, the mice were infected by oral gavage with
170 a high dose of approximately 450 eggs of *T. muris* strain E and observed for up to 30 days post-
171 infection (dpi). Mice were euthanized by cervical dislocation to determine worm counts and
172 other final readouts. A piece (~0.5 cm) of the cecum was fixed in methacarn in order to
173 determine goblet cell numbers. The remaining part of the cecum and 2 cm of the attached colon
174 were frozen at –20 °C to determine *T. muris* worm burden. A piece (~0.5 cm) of the colon was
175 emptied from content, longitudinally cut-opened and weighted before an incubation of 24 h at
176 37 °C, 5 % $CO_2$, in culture medium (RPMI with L-glutamine, 5% fetal bovine serum, 100U
177 penicillin-streptomycin) for analysis of cytokine secretion. The remaining colonic tissue and
178 mesenteric lymph nodes were stored in RNAprotect Tissue Reagent (Qiagen, Hilden,
179 Germany; catalog no. 76106, according to the manufacturer's protocol) or processed for
180 immune cell isolation and FACS analysis. Serum of the euthanized mice was collected and
181 stored at –20 °C.
182
183 ***Parasitological techniques***
184 *T. muris* maintenance and infection was performed as previously described[36]. Mice were orally
185 infected with ~450 eggs and worm burdens were assessed by counting the number of worms
186 present in the cecum and 2 cm of the attached colon on days 20, 25 and 30 post infection, as
187 described previously[36]. The researcher, S.T., who counted the worms, was blinded for both the
188 individual time points and dietary groups.
189
190 ***ELISA***
191 Lipocalin-2 ELISA was performed on stool samples using the lipocalin-2/NGAL DuoSet
192 ELISA R&D system (Bio-Techne, Minneapolis, MN, USA; catalog no. DY1857) according to
193 the manufacturer's instructions and samples were prepared as previously described[31]. MCPT1
194 concentration of serum samples was determined using the MCPT-1 (mMCP-1) Mouse
195 Uncoated ELISA Kit from Invitrogen (Waltham, MA, United States, catalog. no. 88-7503-88)
196 according to manufacturer's instructions. Serum ELISA for total IgG1 and IgE were performed
197 by coating plates using 0.5 µg/µl rat α mouse IgE purified UNLB (Imtec Diagnostics, 1130-
198 01) or rat α-mouse IgG1 purified UNLB (Imtec Diagnostics, Ardmore, OK, United States;
199 catalog no. 1144-01) capture antibody diluted in 0.05 M carbonate/bicarbonate buffer (pH 9.6).
200 Washing steps were performed using 1% Tween, 154 mM NaCl, 10 mM Trizma Base.

201 Blocking of the plates was performed using 1% w/v of BSA in a TBS buffer (15 mM Trizma-
202 acetate, 136 mM NaCl & 2 mM KCl). Mouse IgG1 Isotype Control UNLB (Imtec Diagnostics,
203 Ardmore, OK, United States; catalog no 0102-01) or Mouse IgE Isotype Control (UNLB),
204 Southern Biotech (Imtec Diagnostics, Ardmore, OK, United States; catalog no 0114-01) served
205 as controls. Serum samples were two-fold diluted using the aforementioned TBS buffer with
206 0.1% w/v Tween-20 and 1% BSA. The secondary antibody was Goat anti-mouse IgG1-AP,
207 Southern Biotech (Imtec diagnostics, Ardmore, OK, United States; catalog no 1071-04) or Goat
208 anti-mouse IgE-AP, Southern Biotech (Imtec diagnostics, Ardmore, OK, United States; catalog
209 no 1110-04), respectively. The substrate solution consisting of 0.5 mg/ml phosphate substrate
210 (Sigma-Aldrich, St. Louis, MO, United States; catalog no. S0642-200 TAB) in 1 mM AMP
211 and 0.1 mM $MgCl_2 \cdot 6H_2O$ and plates were read at 405 nm using a SpectraMax ABS PLUS
212 spectrophotometer (Molecular Devices, San Jose, CA, United States). A detailed protocol can
213 be found in the supplementary methods section. Parasite specific IgG1 and IgG2c ELISA was
214 performed as previously described[37].
215
216 ***LEGENDplex bead-based immunoassay***
217 The LEGENDplex assay (BioLegend, San Diego, CA, USA) was performed on serum samples
218 or colon tissue supernatant according to manufacturers' instruction.
219
220 ***RNA extraction and RT-qPCR from mesenteric lymph nodes, colonic tissue***
221 A detailed protocol can be found in the supplemental methods section.
222
223 ***RNA-Seq***
224 RNA extracted from samples at 30 dpi were utilized for performing RNA-Seq. Illumina
225 Stranded Total RNA Prep with Ribo-Zero Plus was used to prepare the RNA sequencing library
226 according to the reference guide's instructions. Sequencing was performed using NovaSeq
227 6000 SP Reagent Kit v1.5 (Illumina, San Diego, CA, USA) on an Illumina NovaSeq 6000
228 system.
229
230 ***Flow cytometry analysis of lamina propria immune cells***
231 Colonic immune cells were isolated using a Lamina Propria Dissociation Kit (Miltenyi Biotec,
232 Bergisch Gladbach, Germany) on the GentleMACS Dissociator (Miltenyi Biotec), following
233 manufacturer's instructions. Cells were washed, counted, and stained as previously described[38].
234 Samples were acquired on a NovoCyte Quanteon flow cytometer (ACEA Biosciences Inc., San

235 Diego, CA, USA). Raw fcs files were analyzed in FlowJo version 10.8.1 as previously
236 described[38].
237
238 ***Statistical analyses***
239 Statistical analysis was performed using Prism 9.2.0. (GraphPad Software, Inc., San Diego,
240 CA, USA). Error bars in all figures represent SEM. Unless specified in the figure legend, a
241 two-way analysis of variance (ANOVA) was performed in Prism and *p* values were adjusted
242 with the original FDR method of Benjamini and Hochberg. P values lower than 0.1 are reported
243 in the figures.
244
245 **Results**
246 ***Dietary fibers tune the worm infection dynamics***
247 We colonized 22-weeks-old germ-free, C57BL/6 mice with a 14-member synthetic human
248 microbiota (14SM), fed them a fiber-rich (FR) or a fiber-free (FF) diet, and then infected them
249 with a high dose of *T. muris* consisting of approximately 450 eggs from the same egg
250 suspension **(Fig. 1A)**. Throughout the experiment, none of the mice exhibited any obvious
251 physiological abnormalities. While FF-fed mice were overall heavier compared to the FR-fed
252 mice, the weights of both groups remained largely stable over time **(Fig. S1A)**. In line with our
253 published work[31,39], the FF diet allowed proliferation of two dominant mucin-degrading
254 bacteria *Akkermansia muciniphila* and *Bacteroides caccae* and reduction of two prominent
255 fiber-degrading bacteria *Eubacterium rectale* and *Bacteroides ovatus* **(Fig. 1B)**. Overall,
256 colonization with the synthetic human microbiota permitted establishment of a low-level *T.*
257 *muris* infection. Interestingly, although the worm burdens were statistically similar between
258 FR and FF groups on 20 and 25 dpi, subsequent infection dynamics significantly differed
259 between both groups, with FF-fed mice clearing the pathogen by 30 dpi and FR-fed mice
260 remaining chronically infected **(Fig. 1C)**.
261
262 In order to investigate whether the two distinct diets and/or the skewed gut microbiome
263 composition toward mucin polymer degradation caused an altered baseline inflammation prior
264 to infection with *T. muris*, we determined fecal lipocalin-2 (LCN-2) levels, which serves as a
265 neutrophilic marker for low-grade inflammation[40]. There were no significant differences
266 between FR and FF groups at day 0, however, after infection, the levels of LCN-2 were
267 significantly higher in the FR group **(Fig. 1D)**.

268

269 ***Diet-driven* T. muris *chronic infection or clearance are supported by Th1 or Th2 immune***
270 ***responses***

271 Chronic *T. muris* infection has been associated with Th1 inflammation while clearance of the
272 worm is usually attributed to a strong Th2 response[2]. To better understand the change in host
273 immunological responses that drive differential *T. muris* infection dynamics, we analyzed the
274 host colonic gene expression at 30 dpi **(Fig. 2A, B, Fig. S1B, C and Table S1)**. We found 147
275 and 184 genes upregulated in the FR- and FF-fed mice, respectively **(Fig. 2A and Tables S2,**
276 **S3)**. Ingenuity Pathway Analysis (IPA) revealed that both the interferon signaling and Th1
277 pathways were upregulated in the FR-fed mice **(Fig. 2B)**, which was consistent with the failure
278 to successfully clear the parasite among FR-fed mice **(Fig. 1C)**. In accordance with the
279 upregulation of the interferon signaling and Th1 pathways, related disease pathways, such as
280 osteoarthritis, systemic lupus erythematosus and even neuroinflammation, were also
281 upregulated as their gene expression profiles overlap with those of a Th1 response **(Fig. 2B)**.
282 Similarly, the Th1 response is potentially linked to the observed increase in antimicrobial
283 responses that results in the activation of cytotoxic T cells, lymphopoiesis, increased apoptosis
284 of macrophages and a reduced replication of viruses **(Fig. S1B)**. In contrast to this, the
285 increased MSP-RON signaling in macrophage pathway hints at a Th2 response under FF
286 conditions **(Fig. 2B),** as an activation of the MSP-RON pathway causes M2 macrophage
287 polarization[41], which is associated with a Th2-type immune response against *T. muris*[42,43].
288 Furthermore, the upregulation of the white adipose tissue browning pathway is also in line with
289 this observation, as M2 macrophage differentiation has been linked to adaptive
290 thermogenesis[44].

291

292 In order to further support conclusions from our RNA-Seq data, we used RT-qPCR to
293 investigate transcript levels of cytokines in mesenteric lymph nodes (MLNs) and colon **(Fig.**
294 **2C, D, Table S4)**. In accordance with the global transcriptome analysis **(Fig. 2A, B)**, the FR-
295 fed mice exhibited a Th1-type response in the MLN, characterized by a peak of *Ifng*, *Tnfa* and
296 *Il1b* transcripts at 25 dpi and a continuously increasing expression of the Th1 transcription
297 factor *Tbet* **(Fig. 2C and Fig. S1D)**. This Th1-type response was also observed in the colon
298 with an increasing expression of *Ifng* over time and a peak of *Tnfa* expression at 25 dpi **(Fig**
299 **2D)**, as well as higher titers of IFNɤ, TNFα and IL-6 in the serum of FR-fed mice at 30 dpi
300 **(Fig. 2E)**. Despite an initial induction of the anti-parasitic Th2-type response in the MLN of
301 FR-fed mice at 15 dpi, *Il13* and *Il4* transcript levels decreased by 20 dpi, consistent with the

302 simultaneous increased expression of the counteracting Th1-type cytokines **(Fig. 2C)**. By
303 contrast, transcript levels of the Th2-type cytokines IL-4, IL-5 and IL-13 and the Th2
304 transcription factor GATA-3 were upregulated over time in either the MLN or colons of FF-
305 fed mice **(Fig. 2D and S1D)**. Further supporting the efficient anti-parasitic response in FF-fed
306 mice, the transcript levels of *Muc2*, the major component of the intestinal mucus, was strongly
307 upregulated in FF-fed mice by 25 and 30 dpi, while remaining low in FR-fed mice **(Fig. 2D)**.
308
309 Assessment of serum concentrations of total IgE and IgG1, both of which are reflective of the
310 protective Th2-type responses against helminths, resulted in no significant changes, albeit an
311 increased trend was observed for both antibodies at 30 dpi **(Fig. S1E)**. We then assessed
312 parasite-specific IgG1 and IgG2, characteristic of Th2 and Th1 responses, respectively[45].
313 Chronic *T. muris* infections are usually characterized by significantly elevated serum levels of
314 parasite-specific IgG2a/c and a low increase in parasite-specific IgG1[45]. In contrast, protection
315 against *T. muris* is characterized by high parasite-specific IgG1 levels, but a lack of IgG2a/c[45].
316 In accordance with the observed worm burdens **(Fig. 1C)**, at 30 dpi, we saw an increase in
317 specific IgG1 in the serum of mice fed the FF diet, while we saw an increase in specific IgG2a/c
318 in mice fed the FR diet **(Fig. 2F)**. Furthermore, serum MCPT1—a proxy for IgE-induced mast
319 cell degranulation[46]—increased at 30 dpi in the FF-fed group **(Fig. 2G)**. These data are in line
320 with an increased tendency of total IgE in the FF-fed group at 30 dpi, and further support the
321 elevated anti-helminth type 2 immunity under fiber deprivation.
322
323 Overall, our data support that worm infection in mice hosting the 14SM and being fed fibers,
324 induce a Th1-type immune response that is driven by an overall increase in IFNγ. On the other
325 hand, in absence of dietary fibers, a similar infectious dose of *T.muris*, induces a Th2-type
326 immune response, resulting in the successful clearance of the worm. We have previously shown
327 that fiber deprivation leads to excessive gut microbial mucin foraging activity[30–32]. Since mucus
328 secretion is essential to the anti-parasitic immunity, and as the gut microbiome is intimately
329 connected to changes in the diet and the host immune responses, we hypothesized that mucin-
330 degrading bacteria promote anti-parasitic immunity.
331
332 ***Mucin-degrading bacteria and absence of fiber promote anti-parasitic immunity***
333 To study the causal mechanism of mucin-degrading bacteria in modulating immunity to
334 helminth infection, we next infected 8-to-12-weeks-old mice, both male and female, colonized
335 with a 10-member synthetic microbiota (10SM) consisting of the 14SM minus the 4 previously

336 characterized mucin-degrading bacteria[31]. In this experiment, 14SM-colonized mice had lower
337 worm burdens compared to the previous experiment (maximum 19 worms versus 53,
338 respectively) (**Fig. 1C and 3A**), and no difference was detected between males and females
339 (data not shown). However, in line with the previous experiment (**Fig. 1C**), the mice fed the
340 FR diet had a higher worm burden than mice on the FF diet which completely cleared the
341 worms by 30 dpi (**Fig. 3A**). The 10SM FR-fed mice harbored worms at all three time points,
342 whereas FF-fed mice presented with few or no worms at any time point (**Fig. 3A**). Nevertheless,
343 all mice developed parasite-specific IgG, confirming that they were properly infected (**Fig.**
344 **3B**). Interestingly, mice fed the FR diet and devoid of mucin-degrading bacteria (10SM FR)
345 had a higher worm burden by 30 dpi compared to 14SM-colonized FR mice (**Fig. 3A**), while
346 they were similar between both groups on 20 and 25 dpi (**Fig. S2A)**. Additionally, among both
347 FF groups at 30 dpi, 10SM-colonized mice had a higher titer of serum specific IgG1 (**Fig. 3B).**
348 On the other hand, among both FR groups at 30 dpi, 10SM-colonized mice had higher amounts
349 of fecal lipocalin-2 **(Fig. S2B**). These data suggest that mucin-degrading bacteria limit worm
350 infection by altering anti-parasitic immunity.
351
352 To better assess the anti-parasitic immune response, we analyzed the immune profiles of
353 mesenteric lymph nodes (MLN) and colons at 20, 25 and 30 dpi. Regardless of bacterial
354 colonization, flow cytometry analysis of immune cell populations in the MLN and colons
355 revealed a higher proportion of Th1 cells in FR-fed mice, in contrast to more Th2 (both MLN
356 and colon) and Treg (colon only) cells in the FF-fed mice (**Fig. 3C, D and S2C**). This diet
357 effect was further supported by transcript and protein expression profiles of Th1-related
358 cytokines (IFNγ, TNFα and IL-1β) in the colons of FR-fed mice and more Th2-related
359 cytokines (IL4, IL-5, IL-9 and IL-13) and MCPT1 in the colons of FF-fed mice (**Fig. 3E and**
360 **S3**).
361
362 Among FR-fed mice, 14SM-colonized mice had lower expression levels of Th1-related
363 cytokine transcripts *Ifng*, *Tnfa* and *Il1b* than 10SM-colonized mice at 30 dpi (**Fig. 3E**).
364 Although these trends were not always consistent at the protein level (**Fig. S3B**), they are
365 perfectly in line with the higher worm burden in 10SM FR mice (**Fig. 3A**), corroborating that
366 the presence of mucin-degrading bacteria further modulates intensity of the anti-parasitic
367 immune response. Among FF-fed mice, 14SM colonization tended to increase the proportion
368 of Th2 cells in the MLN at 25 dpi but then reduced it at 30 dpi in both the MLN and colon (**Fig.**
369 **3C, D**). Supporting an earlier T cell response in 14SM-colonized mice, the colonic transcript

370 levels of the growth factor IL-2 and the Type 2 promoting cytokines IL-25 and IL-33 were
371 already higher at 20 dpi in FF-fed, 14SM-colonized mice compared to FF-fed, 10SM-colonized
372 mice (**Fig. S3A**).
373
374 Intriguingly, FF-fed, 10SM-colonized mice had increased proportions of Tregs, ILC1 and ILC3
375 in the colon at 25 dpi (**Fig. 3D and S2C**), which may impair a timely Th2-driven anti-parasitic
376 response[47]. Further confirming an impaired anti-parasitic response in FF-fed, 10SM-colonized
377 mice, the increased proportion of colonic Th2 and ILC2 at 30 dpi was poorly reflected by IL-
378 5 and IL-13 cytokine production (**Fig. 3D, S2C and S3B**). Consistently, *Muc2* transcript was
379 strongly increased in FF-fed, 14SM-colonized mice but not in 10SM-colonized mice (**Fig. 3E**).
380 Additionally, at 25 dpi, 14SM-colonized FF-fed colons also produced more IL-10 and Th17-
381 related cytokines (IL17-A, IL-17F and IL-22) compared to all other groups (**Fig. S3B**),
382 suggesting a more efficient barrier healing and protective process in the presence of mucin-
383 degrading bacteria and in the absence of dietary fibers. These results strongly support that
384 mucin-degrading bacteria and absence of fiber act together to promote an anti-parasitic immune
385 response.
386
387 ***Mucin-degrading bacteria promote mucus production under fiber deprivation***
388 As a result of a strong type-2 immune response, mucus production is a key mechanism of host
389 defense during parasite infection and can be regulated at the transcriptional, translational and
390 post-translational levels. From 15 to 30 dpi, both FR- and FF-fed 14SM-colonized mice had
391 moderately increased numbers of goblet cells per crypt, but no difference was seen between
392 dietary groups (**Fig. 4A**). Transcriptomic analysis of colon tissues at 30 dpi revealed that the
393 expression of numerous genes involved in mucus production and glycosylation pathways were
394 upregulated in FF-fed mice compared to FR-fed mice (**Fig. 4B**). Moreover, targeted qPCR
395 revealed that, in addition to *Muc2* (**Fig. 2C and 3E**), *Muc5ac* expression was higher in 14SM-
396 colonized FF-fed mice at 30 dpi, compared to FR-fed mice or FF-fed, 10SM-colonized mice
397 (**Fig. 4C**). Similarly, the combination of both mucin-degrading bacteria and fiber deprivation
398 induced the expression of *C1galt1*, *B3gnt6*, *Fut2*, *Galnt3* and *Gal3st2*, which encode key
399 enzymes involved in mucin glycosylation (**Fig. 4C, Table S4**). These results suggest that
400 mucin-degrading bacteria support production of mucus under fiber deprivation, and possibly
401 ensure its proper glycosylation so that this new mucus can be secreted in order to expulse the
402 worms.
403

404 ***Increased mucin–microbiome interactions promote worm clearance***
405 To better understand the role of specific microbiota members in the course of the parasite
406 infection, we first analyzed the composition of the fecal microbiota (**Fig. S4**). Surprisingly and
407 despite the reproducible phenotypes showed above, the 14SM microbiota composition at the
408 time of infection was different between the first experiment (**Figs. 1, 2**) and the second
409 experiment (**Fig. 3**) (**Fig. S4, 5**, **Supplementary results**). The analysis of the relative
410 abundance over time for individual bacteria revealed different profiles between groups with
411 little reproducibility between independent experiments, except for *A. muciniphila* and *B.*
412 *caccae* (**Fig. 5A, B**, **S4B and S6, 7**). Despite different initial relative abundances between the
413 two experiments, these 2 mucin degraders expanded significantly and reproducibly from 14 to
414 20 dpi (**Fig. 5A, B**), a timepoint when mice usually start to expel their worms.
415
416 Consistent with the evolving mucus production and microbiota composition, the enzymatic
417 activities targeting either mucin glycans only (fucosidase and *N*-acetyl-glucosaminidase) or
418 both mucin and dietary glycans (glucosidase) evolved over time during *T. muris* infection (**Fig.**
419 **5C, Tables S5–7**). The activities of mucin-targeting enzymes were higher in 14SM-colonized
420 and FF-fed mice (**Fig. 5C**), and correlated negatively with the worm burden (**Fig. 5D**), further
421 supporting a role for mucin-degrading bacteria in facilitating worm expulsion. Of note,
422 fucosidase activity in 14SM-colonized FF-fed mice (**Fig. 5C**) followed the expression profile
423 of the fucosyltransferase transcript *Fut2* (**Fig. 4C**), decreasing at 25 dpi to increase again by 30
424 dpi, supporting a microbial enzyme activity that may be driven by the glycosylation profile of
425 the mucins. Finally, among the four mucin-degrading strains, the relative abundance of *B.*
426 *caccae* and *A. muciniphila* correlated positively with *N*-acetyl-glucosaminidase activity (**Fig.**
427 **5E and Table S6**), while the relative abundance of *B. thetaiotaomicron* and *B. intestinihominis*
428 correlated negatively with *N*-acetyl-glucosaminidase and fucosidase activities, respectively
429 (**Fig. 5F**, **Tables S5, 6**).
430
431 **Discussion**
432 Helminth infection models have been profoundly utilized to elucidate the underlying host
433 responses for the past several decades, yet open questions remain about the mechanisms of how
434 the intricate interactions between the gut microbiome and GI mucus affect worm infection
435 dynamics including the host immune responses. Here, we shed insight into the role of bacterial
436 mucin foraging in altering the host immune responses during the infection with *T. muris*. Using

437 a functionally characterized synthetic human microbiota that allows either an ablation of
438 microbial mucin foraging or increase in microbial mucin foraging through reduced fiber
439 consumption, our study supports a model in which the mucin-degrading bacteria promote anti-
440 parasitic immunity, that can be further enhanced by reduced dietary fiber **(Fig. 6)**. Our results
441 identify mucin-degrading bacteria as an innovative link in the gut microbiome–parasite axis,
442 suggesting a causal mechanism through which the anti-parasitic immunity is a modulated.
443
444 It is well known that bacteria are important for *T. muris* worm hatching[8,9], although the specific
445 bacterial members involved are not well defined and it is possible that the selected bacteria in
446 our synthetic human microbiota might not be ideal for inducing egg hatching for mouse
447 *Trichuris*, resulting in a lower level of infection of *T. muris* that provides a chronic low-level
448 infection characteristic of infections under natural conditions. Thus, our tractable synthetic
449 microbiota, that facilitates functional interpretations, is a good model to understand the
450 mechanisms linking the worm infection and mucin–microbiome interactions, which would be
451 difficult to decipher in such great detail using a complex, native microbiota. Although the fiber-
452 deficient mice, lacking the mucin-degrading bacteria, contained none to very few worms, these
453 mice still mounted a robust anti-parasitic immune response (**Fig. 3B**). Differences in the
454 parasitic load observed between the two experiments (**Figs. 1, 2 vs. Fig. 3**) could be due to
455 several factors such as the age of the mice used for these experiments (22 weeks vs. 8–12
456 weeks) or in some other unknown factors, yet both experiments provided similar key outcomes.
457 We noticed inconsistency between some readouts e.g., immune cell profiles (MLNs and
458 colons) and serum cytokines at protein level, which is not unexpected for such detailed,
459 complex longitudinal data sets. Nevertheless, overall, the data from our gnotobiotic mouse
460 models allow us to adequately support our main conclusions.
461
462 Our study shows an IFNγ-dominated Th1 response, along with a chronic *T. muris* infection,
463 when mice were fed a normal chow (which we called a fiber-rich (FR) diet), in contrast to a
464 Th2 response and worm clearance under fiber deprivation **(Figs. 1–3 and 6)**. Two previous
465 studies[27,48] observed a similar Th1 response when specific pathogen free mice—containing
466 their native, complex microbiotas—were fed diets containing purified 10% inulin or dried
467 chicory leaves. Nevertheless, these studies did not provide an explanation for the underlying
468 mechanisms. Using our 14SM model, we offer an explanation that the mucin–microbiome
469 interactions driven by dietary changes alter the host immune responses and the worm infection
470 dynamics **(Fig. 6)**. Our study lays groundwork for investigating future molecular mechanisms

471 of how mucolytic bacteria drive specific alterations in mucus glycosylation and how such
472 alterations impact host immune response to worm infection.
473
474 *T. muris* has been shown to broadly alter the host's gut microbiome composition[23–28]. Here,
475 repeating the experiment in several batches of animals revealed different, most likely age-
476 dependent, profiles of microbiota composition over the course of the infection (**Figs. S4–7**).
477 Nevertheless, the infectious phenotype was reproducible as well as a decline of *A. muciniphila*
478 at 15 dpi followed by an expansion of both *A. muciniphila* and *B. caccae* at 20 dpi in fiber-
479 deprived mice (**Fig. 5A, B**). The role of mucin-degrading bacteria such as *A. muciniphila* and
480 *B. caccae* in our model is evident because colonization with a synthetic microbiota without
481 mucin-degrading bacteria prevented the fiber deprivation-induced Th2 immunity (**Fig. 3**).
482
483 In contrast to the observations in *Muc2*$^{-/-}$ mice[29], in our model, increased microbial mucin
484 foraging under fiber-deprived conditions did not delay the parasite clearance, but instead
485 promoted the clearance. These results are not unexpected as genetic ablation of Muc2 largely
486 destabilizes the mucus structure, whereas the increased microbial mucin foraging seems to
487 either resist transition to a Th1 response and aids in a Th2 response. We could not detect an
488 increase in goblet cell numbers/mucin production associated with this (**Fig. 4A**). Nevertheless,
489 we observed increased transcription of genes involved in mucin glycosylation (**Fig. 4B, C**),
490 which has been shown previously to alter susceptibility to *T. muris*[49]. Considering that mucin
491 glycosylations are built-up by the host glycosyltransferases and targeted by the microbial
492 enzymes[50], our results suggest that fiber deprivation promotes changes in mucin glycosylation
493 that facilitates mucus degradation by the fiber-deprived microbiota and aids in clearance of *T.*
494 *muris*.
495
496 Given the high morbidity associated with the parasitic infections in humans[51], our study has
497 generated important prerequisite knowledge for clinical settings: 1) for treating parasitic
498 infections – in the absence of co-infections, periodic fiber deprivation or fasting to boost
499 microbial mucin foraging could be potentially employed in the clinic to manage worm
500 infections; and 2) for harnessing the immunomodulatory properties of helminths for their
501 potential therapeutic use in inflammatory disorders[52] or allograft rejection[53]. Further research
502 is required about how the model proposed in our study **(Fig. 6)** could be translated into the
503 clinic.

504 **References**


505 1. Douglas B, Oyesola O, Cooper MM, et al. Immune System Investigation Using
506 Parasitic Helminths. Annu Rev Immunol 2021;39:639–665.
507 2. Klementowicz JE, Travis MA, Grencis RK. Trichuris muris: A model of
508 gastrointestinal parasite infection. Semin Immunopathol 2012;34:815–828.
509 3. Yousefi Y, Haq S, Banskota S, et al. Trichuris muris model: Role in understanding
510 intestinal immune response, inflammation and host defense. Pathogens 2021;10.
511 4. Colombo SAP, Grencis RK. Immunity to Soil-Transmitted Helminths: Evidence From
512 the Field and Laboratory Models. Front Immunol 2020;11.
513 5. Zaiss MM, Harris NL. Interactions between the intestinal microbiome and helminth
514 parasites. Parasite Immunol 2016;38:5–11.
515 6. Brosschot TP, Reynolds LA. The impact of a helminth-modified microbiome on host
516 immunity review-article. Mucosal Immunol 2018;11:1039–1046.
517 7. Jaenike J, Unckless R, Cockburn SN, et al. Adaptation via symbiosis: Recent spread of
518 a drosophila defensive symbiont. Science (80- ) 2010;329:212–215.
519 8. Hayes KS, Bancroft AJ, Goldrick M, et al. Exploitation of the intestinal microflora by
520 the parasitic nematode trichuris muris. Science (80- ) 2010;328:1391–1394.
521 9. White EC, Houlden A, Bancroft AJ, et al. Manipulation of host and parasite
522 microbiotas: Survival strategies during chronic nematode infection. Sci Adv 2018;4.
523 10. Robertson A, Sall J, Venzon M, et al. Bacterial contact induces polar plug
524 disintegration to mediate whipworm egg hatching. PLOS Pathog 2023;19:e1011647.
525 11. Hewitson JP, Harcus Y, Murray J, et al. Proteomic analysis of secretory products from
526 the model gastrointestinal nematode Heligmosomoides polygyrus reveals dominance
527 of Venom Allergen-Like (VAL) proteins. J Proteomics 2011;74:1573–1594.
528 12. Abner SR, Parthasarathy G, Hill DE, et al. Trichuris suis: Detection of antibacterial
529 activity in excretory-secretory products from adults. Exp Parasitol 2001;99:26–36.
530 13. Su L, Su CW, Qi Y, et al. Coinfection with an intestinal helminth impairs host innate
531 immunity against Salmonella enterica serovar typhimurium and exacerbates intestinal
532 inflammation in mice. Infect Immun 2014;82:3855–3866.
533 14. Fricke WF, Song Y, Wang AJ, et al. Type 2 immunity-dependent reduction of
534 segmented filamentous bacteria in mice infected with the helminthic parasite
535 Nippostrongylus brasiliensis. Microbiome 2015;3:40.
536 15. Forman RA, DeSchoolmeester ML, Hurst RJM, et al. The Goblet Cell Is the Cellular

537 Source of the Anti-Microbial Angiogenin 4 in the Large Intestine Post Trichuris muris
538 Infection. PLoS One 2012;7.
539 16. Shea-Donohue T, Sullivan C, Finkelman FD, et al. The Role of IL-4 in
540 Heligmosomoides polygyrus -Induced Alterations in Murine Intestinal Epithelial Cell
541 Function. J Immunol 2001;167:2234–2239.
542 17. Harris JB, Podolsky MJ, Bhuiyan TR, et al. Immunologic responses to Vibrio cholerae
543 in patients co-infected with intestinal parasites in Bangladesh. PLoS Negl Trop Dis
544 2009;3.
545 18. Kosik-Bogacka DI, Wojtkowiak-Giera A, Kolasa A, et al. Hymenolepis diminuta:
546 Analysis of the expression of Toll-like receptor genes and protein (TLR3 and TLR9) in
547 the small and large intestines of rats. Exp Parasitol 2014;145:61–67.
548 19. Zakeri A, Borji H, Haghparast A. Interaction Between Helminths and Toll-Like
549 Receptors: Possibilities and Potentials for Asthma Therapy. Int Rev Immunol
550 2016;35:219–248.
551 20. Marillier RG, Michels C, Smith EM, et al. IL-4/IL-13 independent goblet cell
552 hyperplasia in experimental helminth infections. BMC Immunol 2008;9.
553 21. Hasnain SZ, McGuckin MA, Grencis RK, et al. Serine Protease(s) Secreted by the
554 Nematode Trichuris muris Degrade the Mucus Barrier. PLoS Negl Trop Dis 2012;6.
555 22. Hasnain SZ, Evans CM, Roy M, et al. Muc5ac: A critical component mediating the
556 rejection of enteric nematodes. J Exp Med 2011;208:893–900.
557 23. Li RW, Wu S, Li W, et al. Alterations in the porcine colon microbiota induced by the
558 gastrointestinal nematode Trichuris suis. Infect Immun 2012;80:2150–2157.
559 24. Broadhurst MJ, Ardeshir A, Kanwar B, et al. Therapeutic Helminth Infection of
560 Macaques with Idiopathic Chronic Diarrhea Alters the Inflammatory Signature and
561 Mucosal Microbiota of the Colon. PLoS Pathog 2012;8.
562 25. Holm JB, Sorobetea D, Kiilerich P, et al. Chronic Trichuris muris infection decreases
563 diversity of the intestinal microbiota and concomitantly increases the abundance of
564 lactobacilli. PLoS One 2015;10.
565 26. Houlden A, Hayes KS, Bancroft AJ, et al. Chronic Trichuris muris infection in
566 C57BL/6 mice causes significant changes in host microbiota and metabolome: Effects
567 reversed by pathogen clearance. PLoS One 2015;10.
568 27. Myhill LJ, Stolzenbach S, Mejer H, et al. Fermentable Dietary Fiber Promotes
569 Helminth Infection and Exacerbates Host Inflammatory Responses. J Immunol
570 2020;204:3042–3055.

571 28. Rosa BA, Snowden C, Martin J, et al. Whipworm-Associated Intestinal Microbiome
572 Members Consistent Across Both Human and Mouse Hosts. Front Cell Infect
573 Microbiol 2021;11.
574 29. Hasnain SZ, Wang H, Ghia JE, et al. Mucin Gene Deficiency in Mice Impairs Host
575 Resistance to an Enteric Parasitic Infection. Gastroenterology 2010;138:1763-1771.e5.
576 30. Neumann M, Steimle A, Grant ET, et al. Deprivation of dietary fiber in specific-
577 pathogen-free mice promotes susceptibility to the intestinal mucosal pathogen
578 Citrobacter rodentium. Gut Microbes 2021;13.
579 31. Desai MS, Seekatz AM, Koropatkin NM, et al. A Dietary Fiber-Deprived Gut
580 Microbiota Degrades the Colonic Mucus Barrier and Enhances Pathogen
581 Susceptibility. Cell 2016;167:1339-1353.e21.
582 32. Parrish A, Boudaud M, Grant ET, et al. Akkermansia muciniphila exacerbates food
583 allergy in fibre-deprived mice. Nat Microbiol 2023 810 2023;8:1863–1879.
584 33. Martens EC, Neumann M, Desai MS. Interactions of commensal and pathogenic
585 microorganisms with the intestinal mucosal barrier. Nat Rev Microbiol 2018;16:457–
586 470.
587 34. Parrish A, Boudaud M, Kuehn A, et al. Intestinal mucus barrier: a missing piece of the
588 puzzle in food allergy. Trends Mol Med 2022;28:36–50.
589 35. Steimle A, Sciscio A De, Neumann M, et al. Constructing a gnotobiotic mouse model
590 with a synthetic human gut microbiome to study host–microbe cross talk. STAR
591 Protoc 2021;2:100607.
592 36. Wakelin D. Acquired immunity to Trichuris muris in the albino laboratory mouse.
593 Parasitology 1967;57:515–524.
594 37. Hayes KS, Cliffe LJ, Bancroft AJ, et al. Chronic Trichuris muris infection causes
595 neoplastic change in the intestine and exacerbates tumour formation in APC min/+
596 mice. PLoS Negl Trop Dis 2017;11.
597 38. Grant ET, Boudaud M, Muller A, et al. Maternal diet and gut microbiome composition
598 modulate early-life immune development. EMBO Mol Med 2023;15.
599 39. Wolter M, Steimle A, Parrish A, et al. Dietary Modulation Alters Susceptibility to
600 Listeria monocytogenes and Salmonella Typhimurium with or without a Gut
601 Microbiota. mSystems 2021;6:e00717-21.
602 40. Chassaing B, Srinivasan G, Delgado MA, et al. Fecal Lipocalin 2, a Sensitive and
603 Broadly Dynamic Non-Invasive Biomarker for Intestinal Inflammation Bereswill S,
604 ed. PLoS One 2012;7:e44328.

605 41. Chaudhuri A. Regulation of macrophage polarization by RON receptor tyrosine kinase
606 signaling. Front Immunol 2014;5.
607 42. Forman R, Logunova L, Smith H, et al. Trichuris muris infection drives cell-intrinsic
608 IL4R alpha independent colonic RELMα+ macrophages. PLoS Pathog 2021;17.
609 43. Sorobetea D, Svensson-Frej M, Grencis R. Immunity to gastrointestinal nematode
610 infections. Mucosal Immunol 2018;11:304–315.
611 44. Hallowell RW, Collins SL, Craig JM, et al. MTORC2 signalling regulates M2
612 macrophage differentiation in response to helminth infection and adaptive
613 thermogenesis. Nat Commun 2017;8.
614 45. Else KJ, Entwistle GM, Grencis RK. Correlations between worm burden and markers
615 of Th1 and Th2 cell subset induction in an inbred strain of mouse infected with
616 Trichuris muris. Parasite Immunol 1993;15:595–600.
617 46. Kasakura K, Nagata K, Miura R, et al. Cooperative Regulation of the Mucosal Mast
618 Cell–Specific Protease Genes Mcpt1 and Mcpt2 by GATA and Smad Transcription
619 Factors. J Immunol 2020;204:1641–1649.
620 47. Hepworth MR, Monticelli LA, Fung TC, et al. Innate lymphoid cells regulate CD4+ T-
621 cell responses to intestinal commensal bacteria. Nat 2013 4987452 2013;498:113–117.
622 48. Valente AH, Jensen KMR, Myhill LJ, et al. Dietary non-starch polysaccharides impair
623 immunity to enteric nematode infection. BMC Biol 2023;21:1–16.
624 49. Hasnain SZ, Dawson PA, Lourie R, et al. Immune-driven alterations in mucin
625 sulphation is an important mediator of Trichuris muris helminth expulsion. PLoS
626 Pathog 2017;13.
627 50. Arike L, Holmén-Larsson J, Hansson GC. Intestinal Muc2 mucin O-glycosylation is
628 affected by microbiota and regulated by differential expression of glycosyltranferases.
629 Glycobiology 2017;27:318–328.
630 51. World Health Organization. Global Health Estimates 2020: Disease burden by Cause,
631 Age, Sex, by Country and by Region, 2000-2019. 2020.
632 52. Helmby H. Human helminth therapy to treat inflammatory disorders- where do we
633 stand? BMC Immunol 2015;16.
634 53. Kiss M, Burns H, Donnelly S, et al. Effectiveness of Helminth Therapy in the
635 Prevention of Allograft Rejection: A Systematic Review of Allogeneic
636 Transplantation. Front Immunol 2020;11.
637
638

639 **Figure legends**

640 **Figure 1. Diet drives changes in mucin-degrading bacteria expansion and alters worm**
641 **infection.**

642 (A) Experimental timeline.

643 (B) Relative bacterial abundance at the time of infection (day 0), determined by qPCR on fecal
644 DNA. Red latin crosses denote known mucin-degrading bacteria.

645 (C) Worm burdens assessed at 20, 25 and 30 dpi. Each dot represents a mouse (n=4–5).
646 Multiple Mann-Whitney test, *p* values adjusted with the FDR method of Benjamini and
647 Hochberg.

648 (D) Fecal Lipocalin-2 (LCN-2) levels assessed by ELISA before (day 0) and after infection
649 with *T. muris* (13, 15, 20, 23, 30 dpi) (n=4–5). *p* values indicate comparisons between FR and
650 FF groups.

651

652 **Figure 2. Dietary fibers skew the anti-parasitic immune response towards Th1-type**
653 **responses.**

654 (A, B) Analysis of data generated by RNA-seq of RNA extracted from colonic tissue at 30 dpi
655 (n=4). (A) Volcano plot of the distribution of all differentially expressed genes. (B) Barplot
656 showing significantly up- or downregulated host pathways ((Fiber Rich (FR)/Fiber Free (FF))
657 determined by Ingenuity Pathway Analysis (IPA). The higher the opacity of the bar, the more
658 up- or downregulated the pathway.

659 (C, D) Relative expression of indicated transcripts in (C) mesenteric lymph nodes and (D)
660 colonic tissue over time after *T. muris* infection (n=3–5); *p* values indicate comparisons
661 between FR and FF groups.

662 (E) Serum cytokine concentrations at 30 dpi (n=4–5). Unpaired, two-tailed t-test.

663 (F) Parasite-specific IgG1 and IgG2a/c concentrations in mouse serum (n=4–5).

664 (G) Serum mast cell protease 1 (MCPT1) concentrations (n=2–5); *p* values indicate
665 comparisons between FR and FF groups.

666

667 **Figure 3. Mucin-degrading bacteria promote the anti-parasitic immunity.**

668 (A) Worm burdens assessed at 20, 25 and 30 dpi in 14SM- and 10SM-colonized mice fed a
669 fiber-rich (FR) or a fiber-free (FF) diet (n=5–6).

670 (B) Parasite-specific IgG1 and IgG2a/c concentrations in mouse serum (n=5–6). *P* values
671 indicate comparisons between FR and FF groups among 10SM- or 14SM-colonized mice.

672 (C, D) Proportion of indicated immune cell populations in (C) the mesenteric lymph nodes
673 and (D) colonic tissue (n=3–6).
674 (E) Relative expression of indicated transcripts in colonic tissue (n=3–6).
675
676 **Figure 4. Mucin-degrading bacteria promote mucus production under fiber deprivation.**
677 (A) Goblet cell counts per crypt of *T. muris* infected mice determined by histological
678 assessment of methacarn-fixed cecum sections (n=2–5).
679 (B) Relative gene expression (FF/FR) at 30 dpi of the 5 most significant activated pathways in
680 the colonic tissue under FF conditions (n=4 per group). Pathways are based on GO terms for
681 biological processes and REVIGO was used to reduce redundant terms.
682 (C) Relative expression of indicated transcripts in colonic tissue (n=2–6).
683
684 **Figure 5. Increased mucin–microbiome interactions promote worm clearance.**
685 (A, B) Relative abundance of *B. caccae* (A) and *A. muciniphila* (B) over the course of *T. muris*
686 infection in 14SM-colonized mice (n=2–6). Significance labels indicate comparisons between
687 FR versus FF groups (black), or between indicated timepoints among FF-fed mice of Fig. 1–2
688 (yellow), FR-fed mice of Fig. 3 (green) and FF-fed mice of Fig. 3 (red).
689 (C) Glycan-degrading enzyme activities of the gut microbiome determined by stool-based p-
690 nitrophenyl glycoside-based enzyme assays. α-fucosidase and β-N-acetyl-glucosaminidase are
691 key mucin-degrading enzymes, while β-glucosidase serves as a control for general glycan-
692 degrading activity (n=3–6). Significance labels indicate comparisons between $^{\&}$FR versus FF
693 groups among 14SM-colonized mice from Figs. 1, 2, *FR versus FF groups among 14SM-
694 colonized mice from Fig. 3, $^{\$}$FR versus FF groups 10SM-colonized mice from Fig.3, and
695 $^{\#}$10SM versus 14SM groups among FF-fed mice. $^{\&}$/*/$^{\#}$p<0.05; $^{\&\&}$/$^{\$\$}$/$^{\#\#}$p<0.01; ***p<0.001;
696 $^{\&\&\&\&}$/****/$^{\$\$\$\$}$/$^{\#\#\#\#}$p<0.0001.
697 (D, E) Spearman correlations between indicated bacteria relative abundance and (D) N-acetyl-
698 glucosaminidase activity (n = 41–70) or (E) fucosidase activity (n = 40).
699 (F) Spearman correlations between worm burdens and enzymatic activities (n=31).
700
701 **Figure 6. Model for the role of mucin-degrading bacteria in facilitating anti-parasitic**
702 **immunity and *T. muris* clearance.**
703 (1) Fiber deprivation promotes microbial mucus foraging and thinning, which may facilitate
704 hatching of the worm to the epithelium and its sensing by the host. (2) This sensing induces a
705 strong type-2 response, leading to mucus production and preventing the worm to stay and

706 develop. (3) Under fiber deprivation the worms reaching the epithelium promote an IFNg
707 response, which inhibits the anti-parasitic response and allows the worm to settle and grow.

# Figure 1. Diet drives changes in mucin-degrading bacteria and alters worm infection.

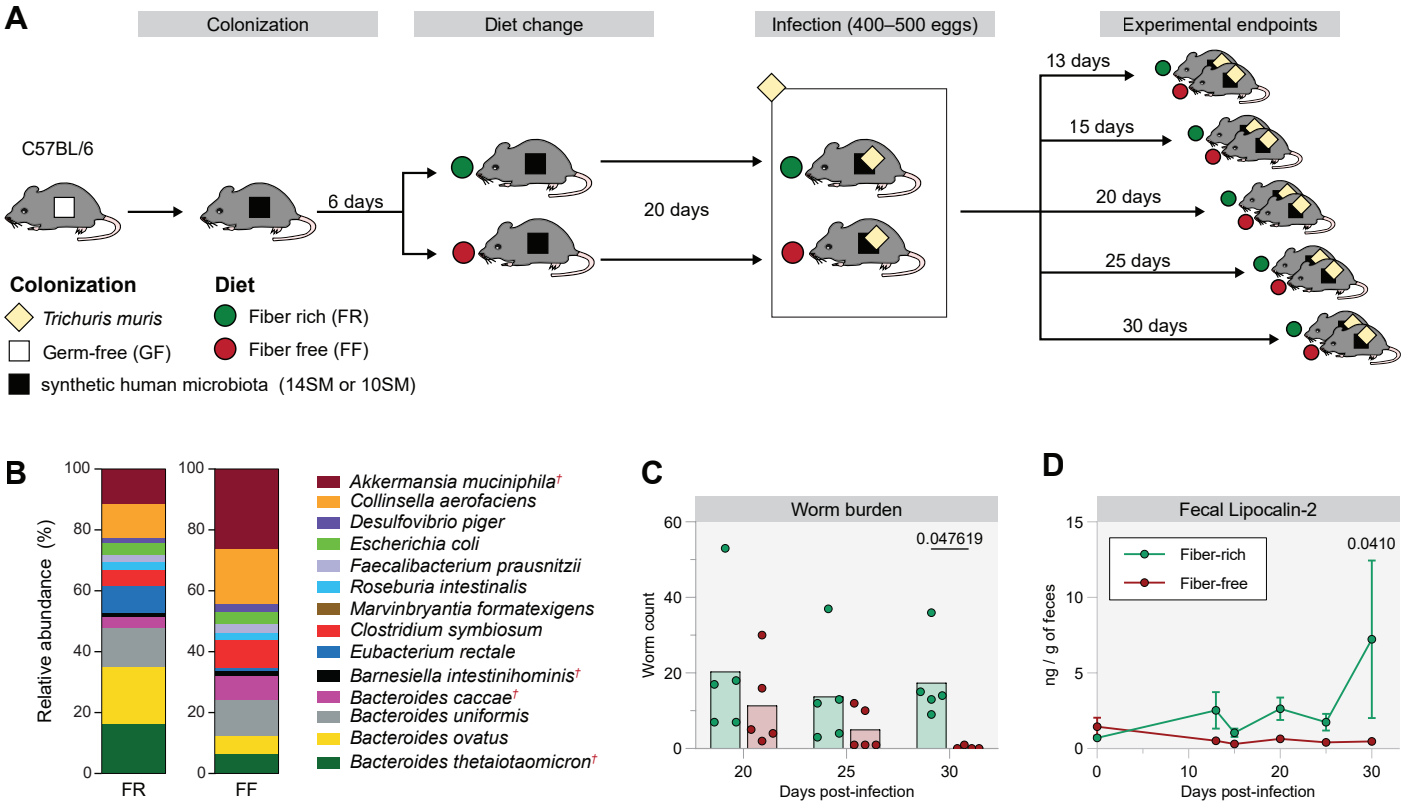

Figure 2. Dietary fiber skew the anti-parasitc immune response towards Th1-type responses.

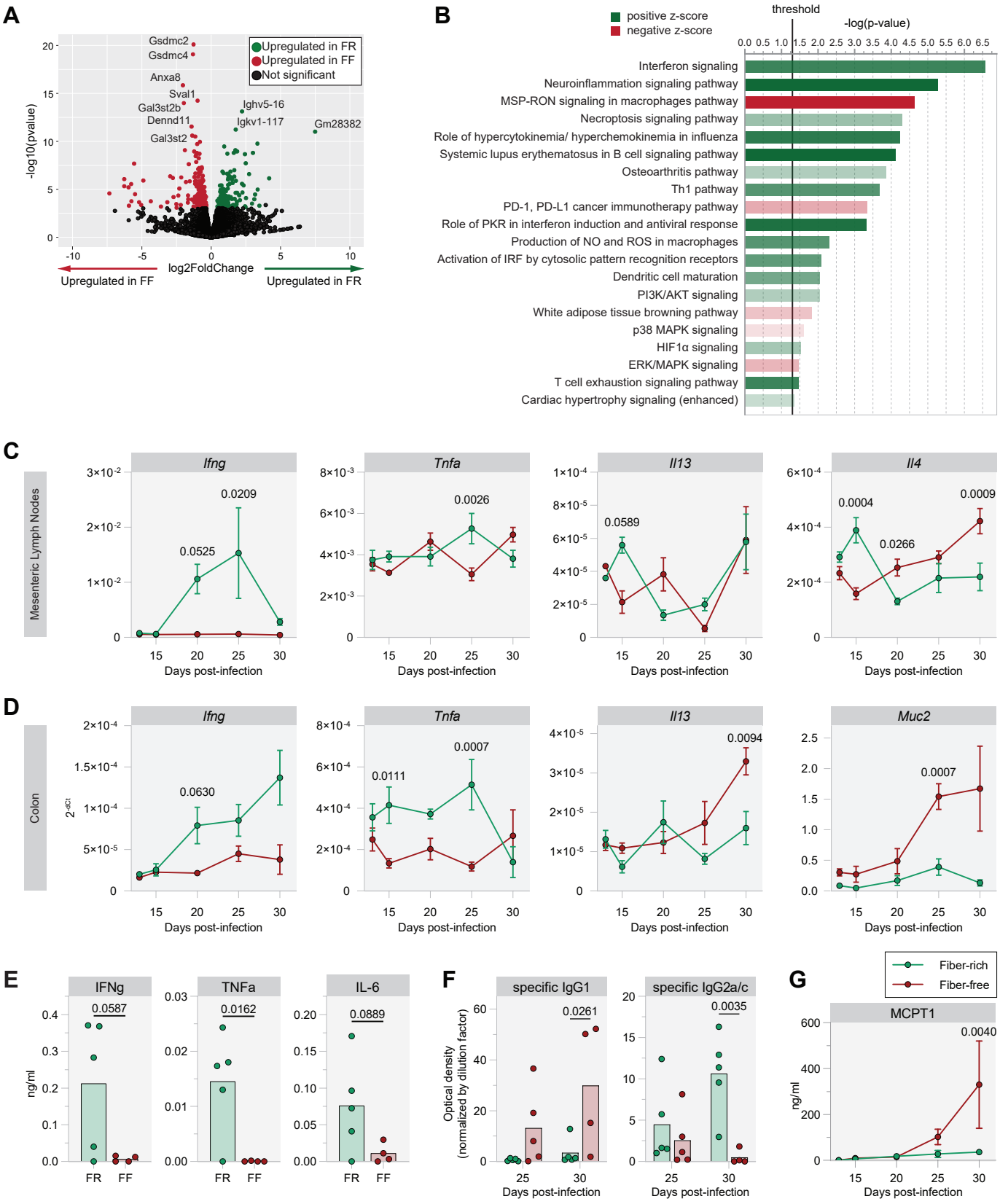

# Figure3. Mucin-degrading bacteria promote the anti-parasitic immunity.

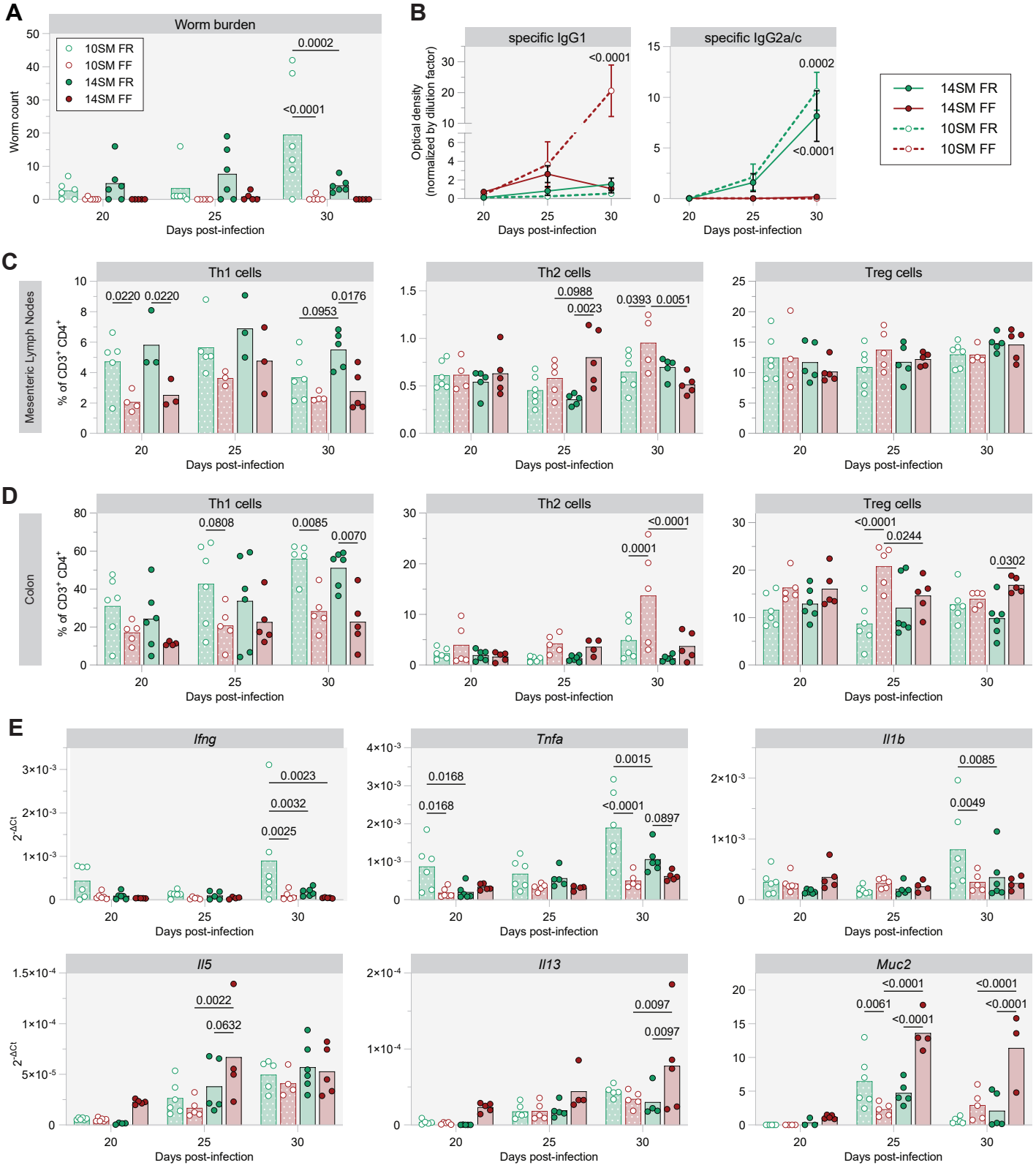

# Figure 4. Mucin-degrading bacteria mediate mucus production under fiber deprivation.

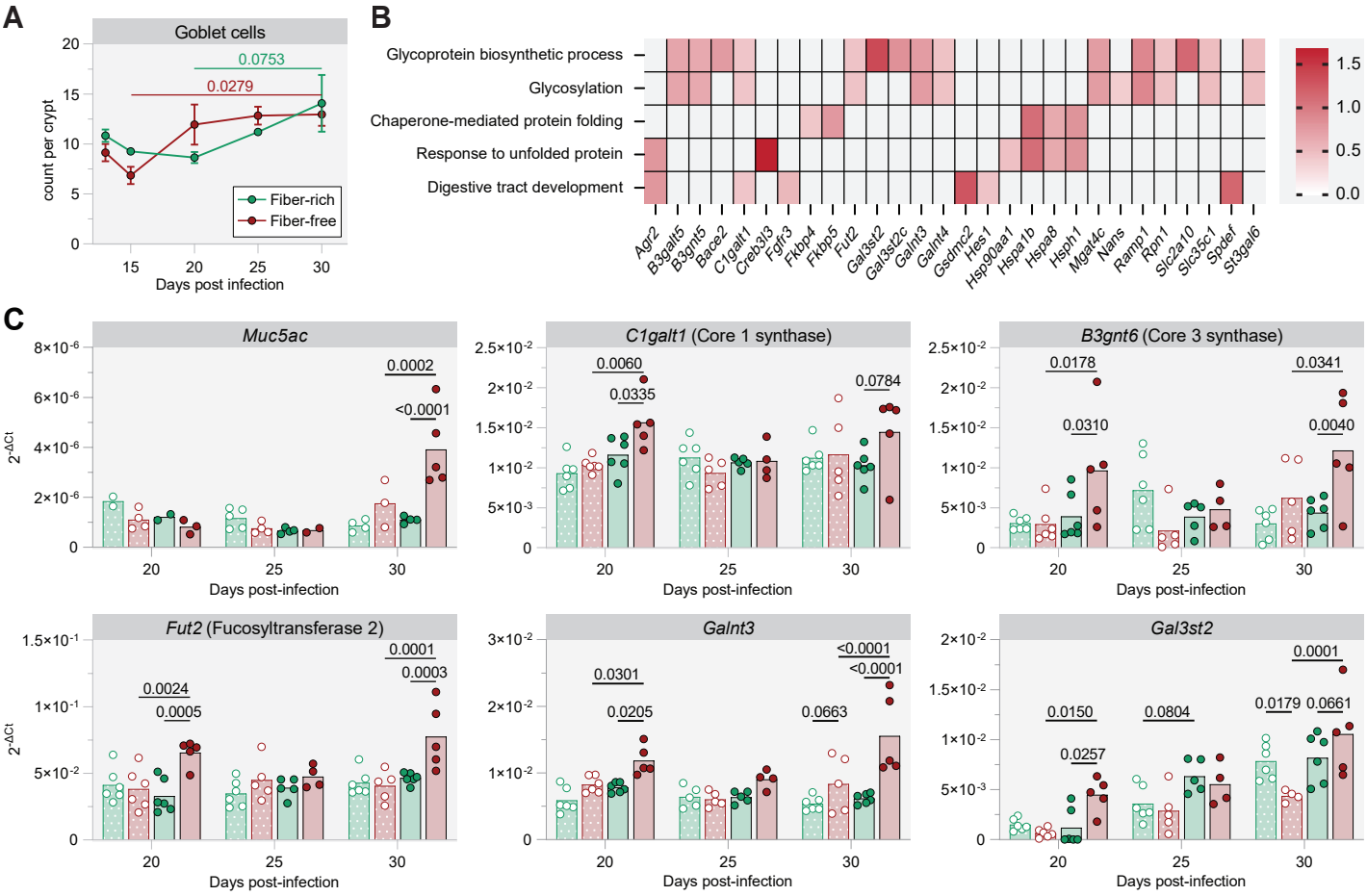

Figure 5. Increased mucin–microbiome interactions promote worm clearance.

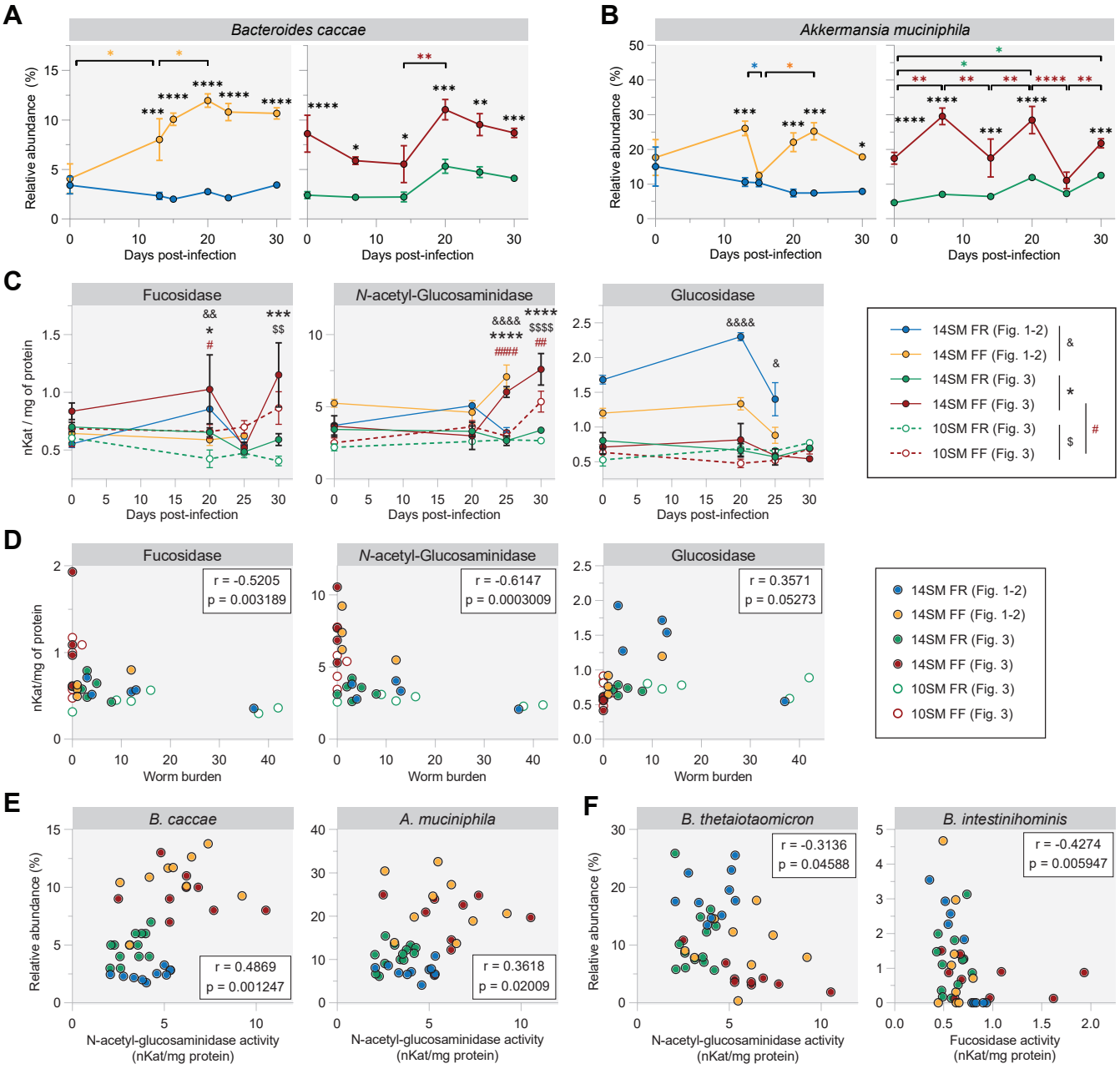

Fig. 6

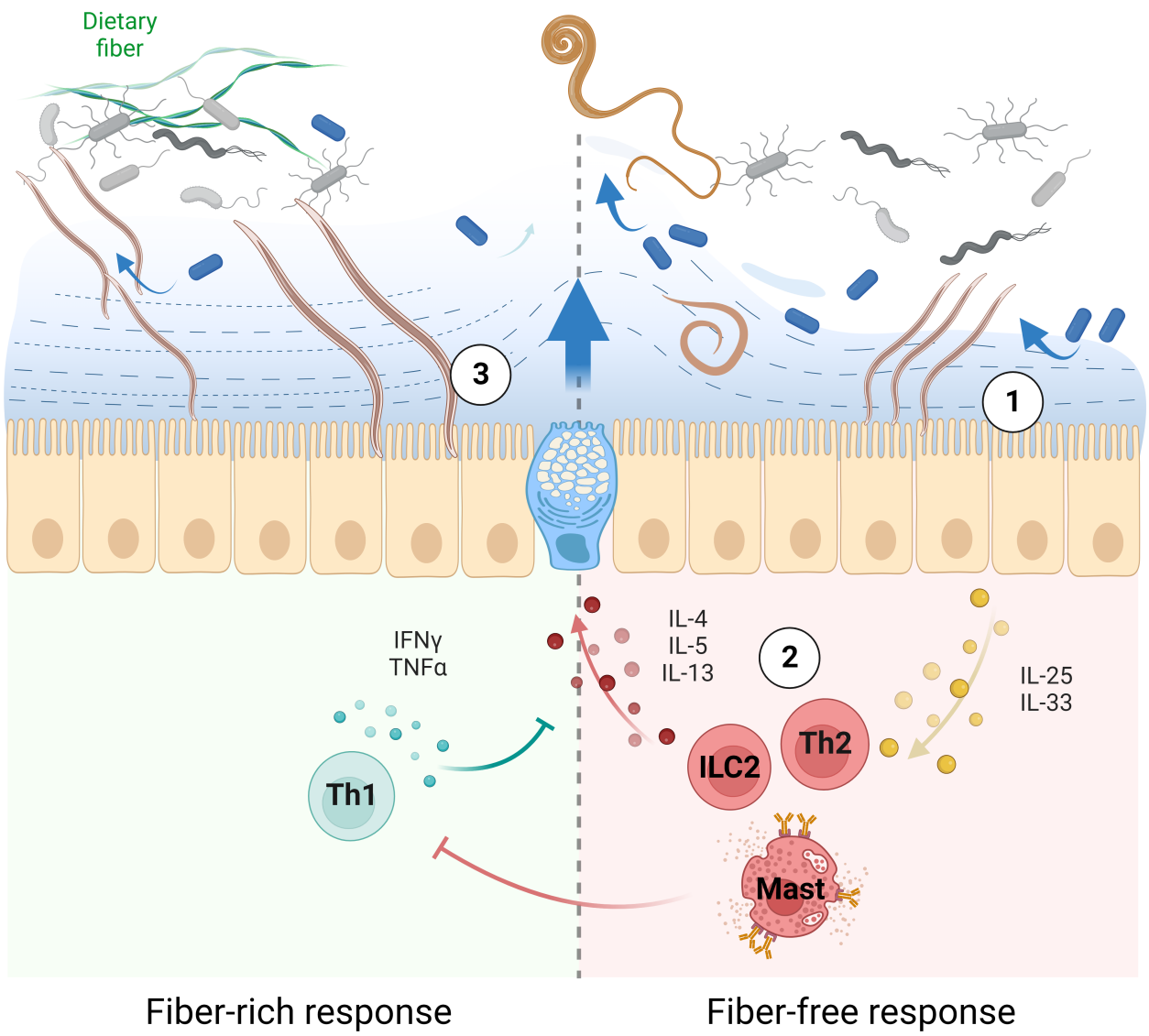
Dietary
fiber
3
1
IFNγ
TNFα
Th1
IL-4
IL-5
IL-13
2
ILC2
Th2
IL-25
IL-33
Mast
Fiber-rich response
Fiber-free response

# Fig. S1

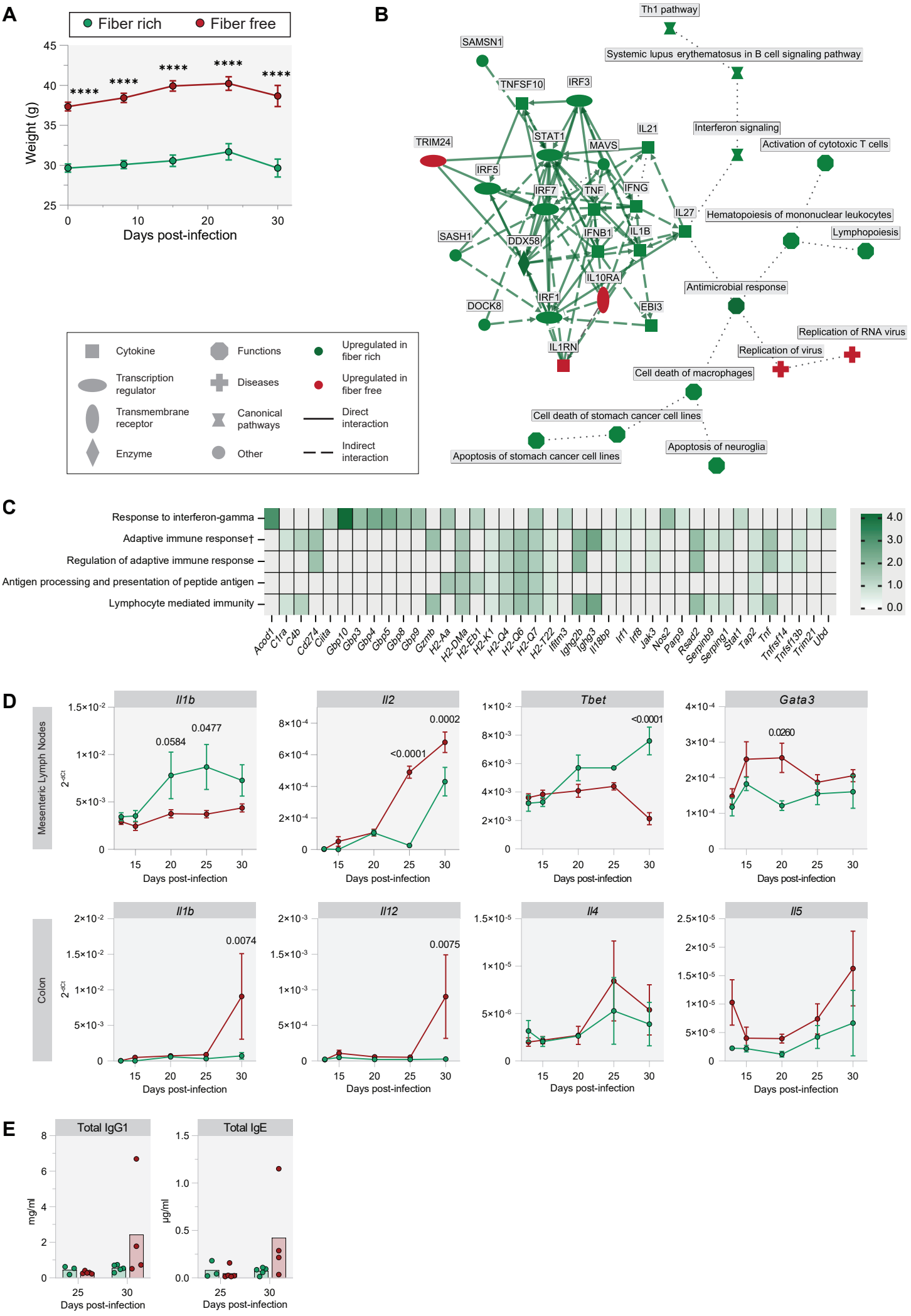
A
Fiber rich
Fiber free
Weight (g)
Days post-infection
B
Th1 pathway
Systemic lupus erythematosus in B cell signaling pathway
Interferon signaling
Activation of cytotoxic T cells
Hematopoiesis of mononuclear leukocytes
Lymphopoiesis
Antimicrobial response
Replication of RNA virus
Replication of virus
Cell death of macrophages
Cell death of stomach cancer cell lines
Apoptosis of stomach cancer cell lines
Apoptosis of neuroglia
SAMSN1
TNFSF10
IRF3
TRIM24
STAT1
MAVS
IL21
IRF5
IRF7
TNF
IFNG
IL27
SASH1
DDX58
IFNB1
IL1B
IL10RA
IRF1
DOCK8
EBI3
IL1RN
Cytokine
Transcription regulator
Transmembrane receptor
Enzyme
Functions
Diseases
Canonical pathways
Other
Upregulated in fiber rich
Upregulated in fiber free
Direct interaction
Indirect interaction
C
Response to interferon-gamma
Adaptive immune response†
Regulation of adaptive immune response
Antigen processing and presentation of peptide antigen
Lymphocyte mediated immunity
Acod1 C1ra C4b Cd274 Ciita Gbp10 Gbp3 Gbp4 Gbp5 Gbp8 Gbp9 Gzmb H2-Aa H2-DMa H2-Eb1 H2-K1 H2-Q4 H2-Q6 H2-Q7 H2-T22 Ifitm3 Ighg2b Ighg3 Il18bp Irf1 Irf8 Jak3 Nos2 Parp9 Rsad2 Serpinb9 Serping1 Stat1 Tap2 Tnf Tnfsf14 Tnfsf13b Trim21 Ubd
D
Mesenteric Lymph Nodes
Il1b
Il2
Tbet
Gata3
0.0584
0.0477
0.0002
<0.0001
<0.0001
0.0260
Days post-infection
Colon
Il1b
Il12
Il4
Il5
0.0074
0.0075
E
Total IgG1
Total IgE
mg/ml
µg/ml
Days post-infection

Fig. S2

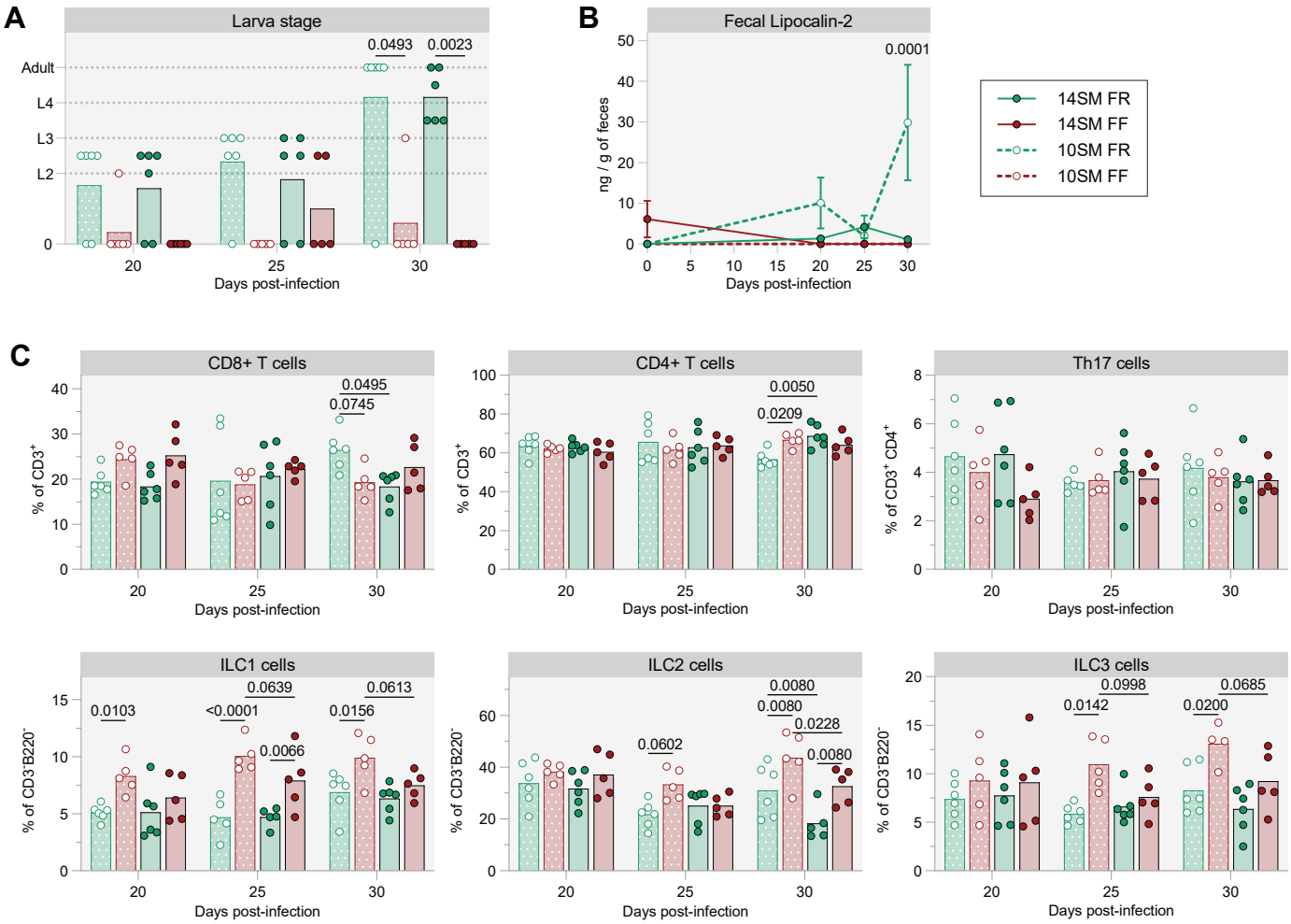
A
Larva stage
Adult
L4
L3
L2
0
0.0493
0.0023
20
25
30
Days post-infection
B
Fecal Lipocalin-2
ng / g of feces
0.0001
Days post-infection
14SM FR
14SM FF
10SM FR
10SM FF
C
CD8+ T cells
% of CD3+
0.0495
0.0745
CD4+ T cells
% of CD3+
0.0050
0.0209
Th17 cells
% of CD3+ CD4+
ILC1 cells
% of CD3-B220-
0.0103
<0.0001
0.0639
0.0066
0.0156
0.0613
ILC2 cells
% of CD3-B220-
0.0602
0.0080
0.0080
0.0228
0.0080
ILC3 cells
% of CD3-B220-
0.0142
0.0998
0.0200
0.0685
Days post-infection

Fig. S3

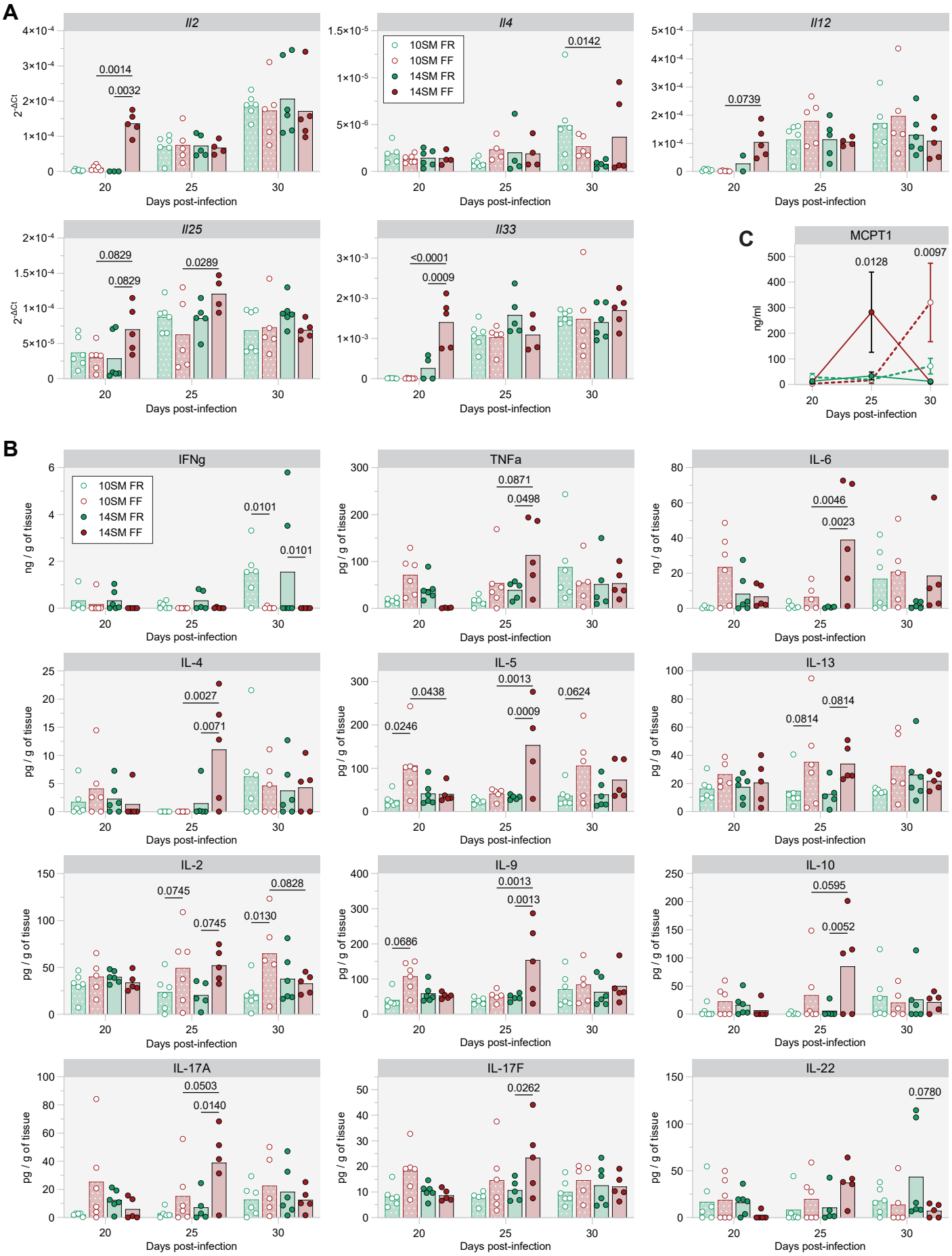
A
Il2
Il4
Il12
Il25
Il33
10SM FR
10SM FF
14SM FR
14SM FF
0.0014
0.0032
0.0142
0.0739
0.0829
0.0829
0.0289
<0.0001
0.0009
2^-ΔCt
Days post-infection
C
MCPT1
0.0128
0.0097
ng/ml
B
IFNg
TNFa
IL-6
IL-4
IL-5
IL-13
IL-2
IL-9
IL-10
IL-17A
IL-17F
IL-22
ng / g of tissue
pg / g of tissue
0.0101
0.0101
0.0871
0.0498
0.0046
0.0023
0.0027
0.0071
0.0438
0.0246
0.0013
0.0009
0.0624
0.0814
0.0814
0.0745
0.0745
0.0828
0.0130
0.0686
0.0013
0.0013
0.0595
0.0052
0.0503
0.0140
0.0262
0.0780

# Fig. S4

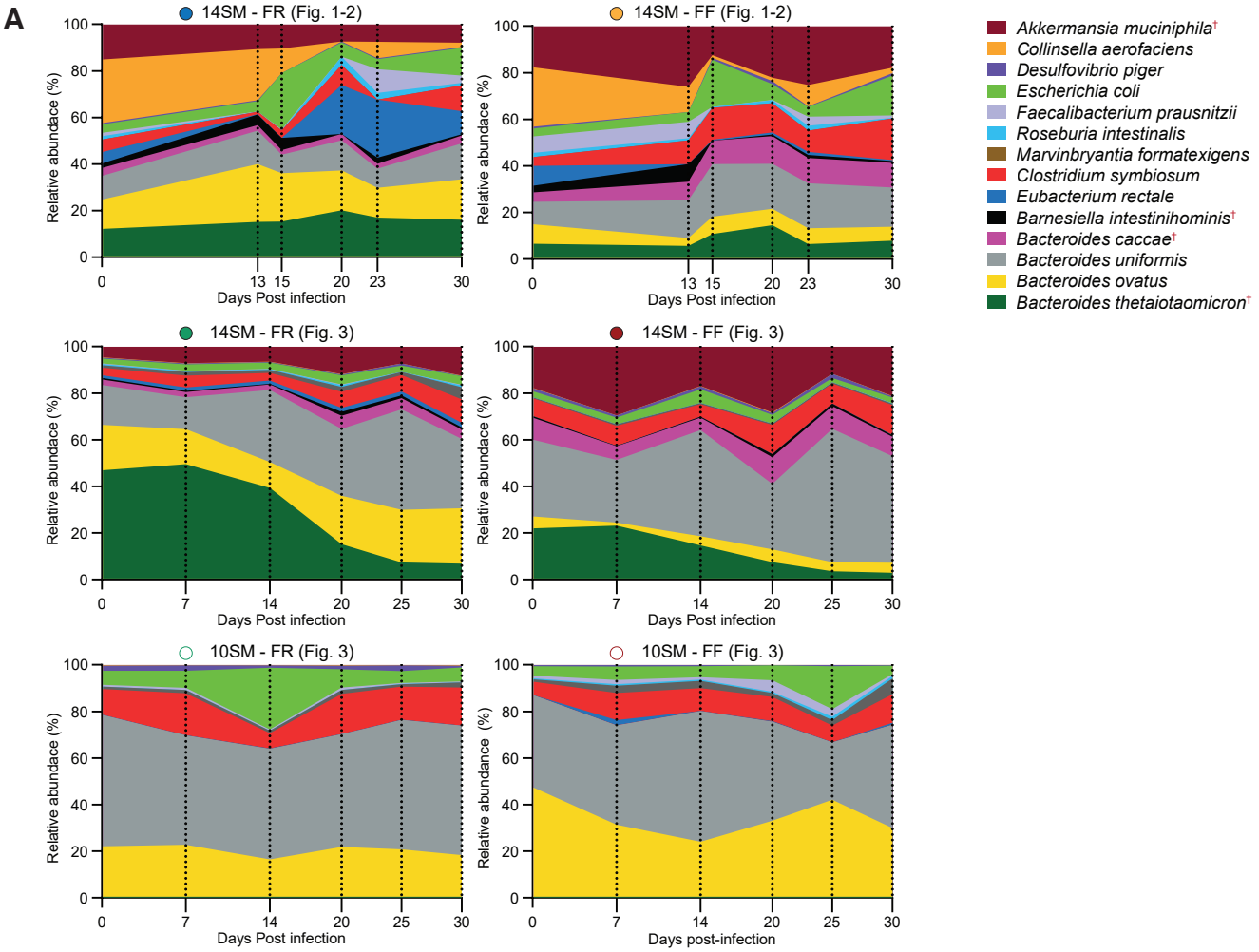
A
14SM - FR (Fig. 1-2)
14SM - FF (Fig. 1-2)
14SM - FR (Fig. 3)
14SM - FF (Fig. 3)
10SM - FR (Fig. 3)
10SM - FF (Fig. 3)
Relative abundace (%)
Relative abundance (%)
Days Post infection
Days post-infection
Akkermansia muciniphila†
Collinsella aerofaciens
Desulfovibrio piger
Escherichia coli
Faecalibacterium prausnitzii
Roseburia intestinalis
Marvinbryantia formatexigens
Clostridium symbiosum
Eubacterium rectale
Barnesiella intestinihominis†
Bacteroides caccae†
Bacteroides uniformis
Bacteroides ovatus
Bacteroides thetaiotaomicron†

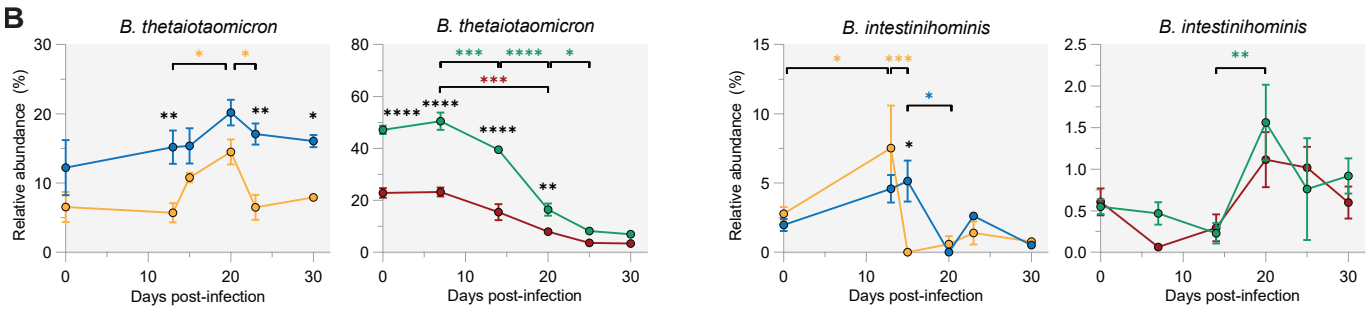
B
B. thetaiotaomicron
B. thetaiotaomicron
B. intestinihominis
B. intestinihominis
Relative abundance (%)
Days post-infection

Fig. S5

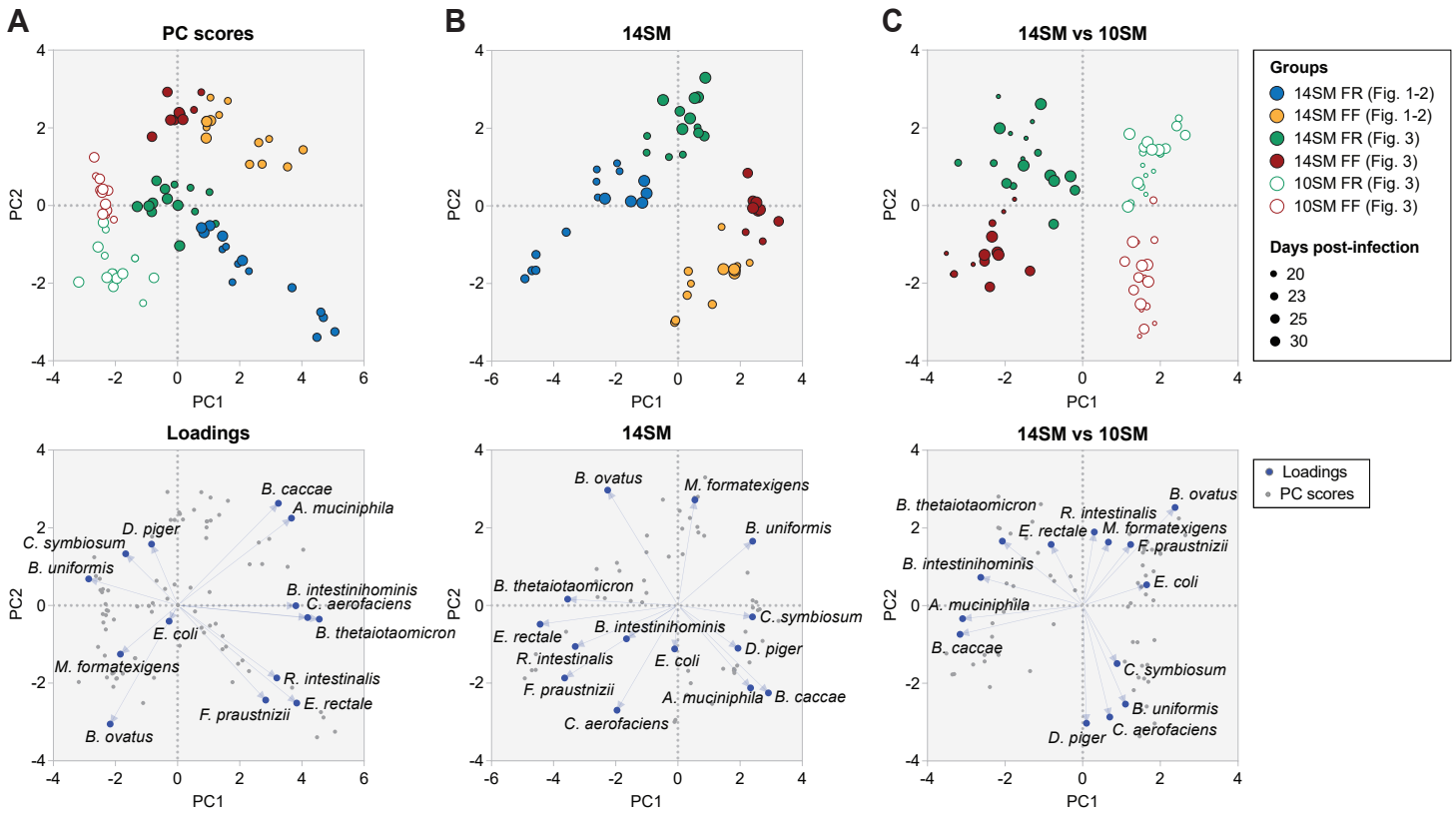
A
PC scores
B
14SM
C
14SM vs 10SM
PC1
PC2
Groups
14SM FR (Fig. 1-2)
14SM FF (Fig. 1-2)
14SM FR (Fig. 3)
14SM FF (Fig. 3)
10SM FR (Fig. 3)
10SM FF (Fig. 3)
Days post-infection
20
23
25
30
Loadings
PC scores
B. caccae
A. muciniphila
D. piger
C. symbiosum
B. uniformis
B. intestinihominis
C. aerofaciens
B. thetaiotaomicron
E. coli
M. formatexigens
R. intestinalis
E. rectale
F. praustnizii
B. ovatus

# Fig. S6

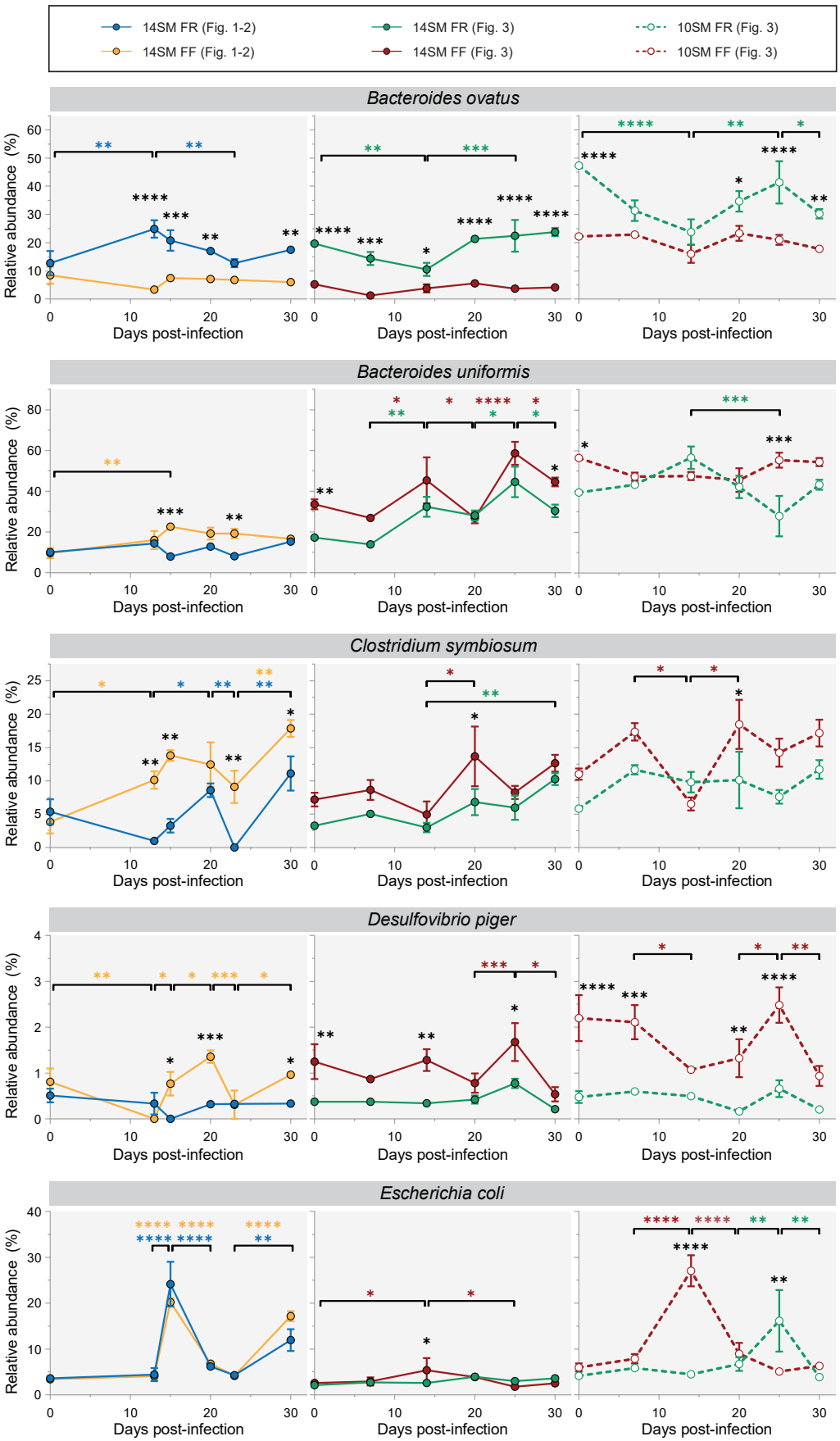
14SM FR (Fig. 1-2)
14SM FF (Fig. 1-2)
14SM FR (Fig. 3)
14SM FF (Fig. 3)
10SM FR (Fig. 3)
10SM FF (Fig. 3)
Bacteroides ovatus
Bacteroides uniformis
Clostridium symbiosum
Desulfovibrio piger
Escherichia coli
Relative abundance (%)
Days post-infection

Fig. S7

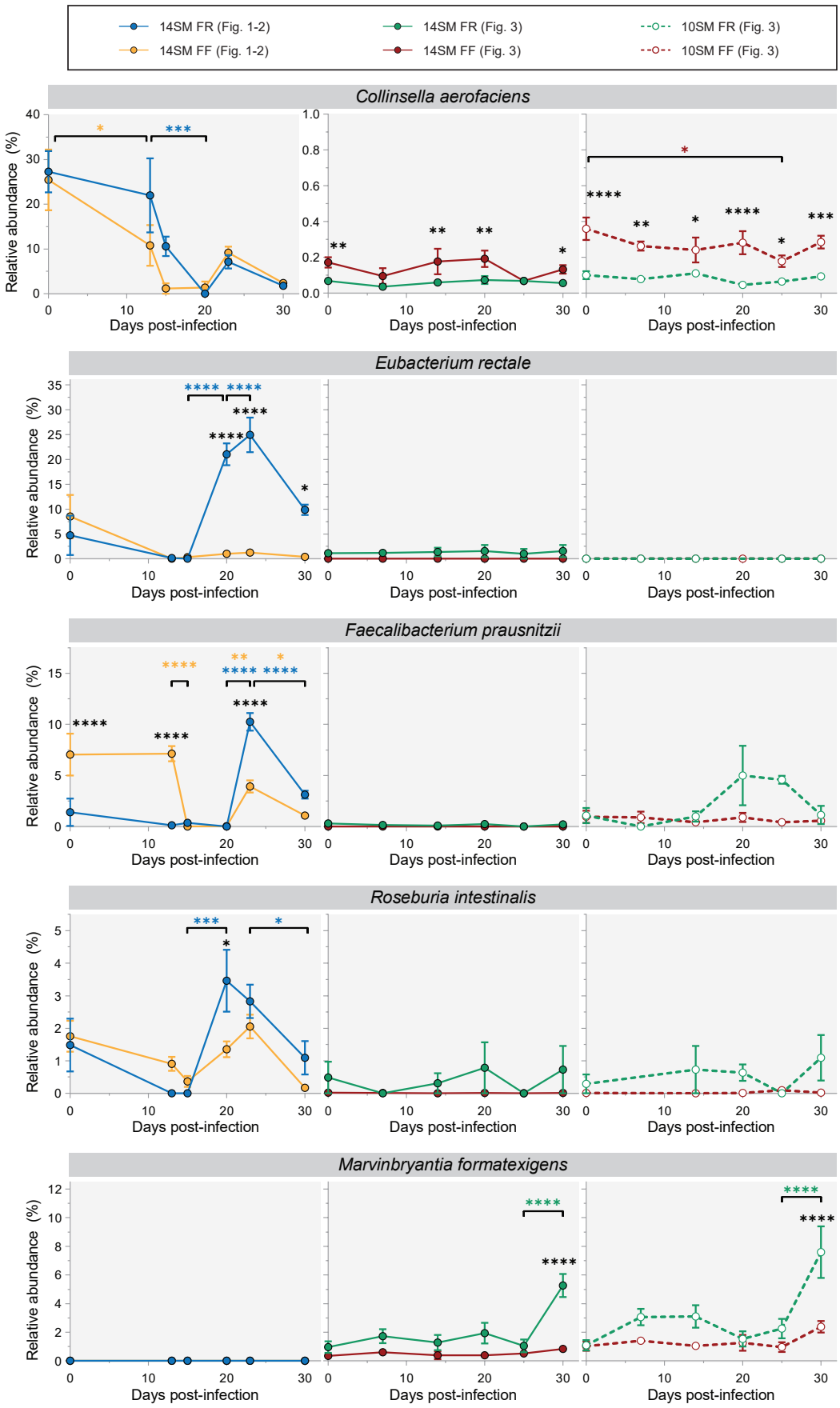
14SM FR (Fig. 1-2)
14SM FF (Fig. 1-2)
14SM FR (Fig. 3)
14SM FF (Fig. 3)
10SM FR (Fig. 3)
10SM FF (Fig. 3)
Collinsella aerofaciens
Eubacterium rectale
Faecalibacterium prausnitzii
Roseburia intestinalis
Marvinbryantia formatexigens
Relative abundance (%)
Days post-infection